Nitric Oxide in the Olfactory Epithelium

Von dem Fachbereich Biologie der Universität Hannover

zur Erlangung des Grades eines

Doktors der Naturwissenschaften

Dr. rer. nat.

genehmigte Dissertation

von

Dipl.-Biol. Oliver Schmachtenberg

geboren am 12. Dezember 1970 in Rüsselsheim

2001

Referent: Prof. Dr. Gerd Bicker

Korreferent: Prof. Dr. Juan Bacigalupo

Dritter Referent: PD Dr. C. Zeilinger

Tag der Promotion: 25. Juni 2001

Zusammenfassung

Die Riechsinneszellen des olfaktorischen Epithels werden lebenslang kontinuierlich erneuert. Jedes neu heranwachsende Neuron schickt dabei einen Dendrit zur Schleimhautoberfläche, um dort Zilien auszubilden, und sein Axon muss zu dem richtigen Glomerulus im olfaktorischen Bulbus finden, um Synapsen zu formen. Eine Expression des Enzyms Stickstoffmonoxid (NO) Synthase wurde während der Embryonalentwicklung und der Bulbektomie-induzierten Regeneration von Riechsinneszellen beobachtet, was auf eine Rolle von NO beim axonalen Auswachsen und der Synaptogenese hindeutet. Der Funktionsmechanismus von NO und die Frage, ob es auch im normalen reifen Riechsinnesepithel eine Rolle spielt, sind jedoch ungeklärt.

In der vorliegenden Arbeit wurde dieses Thema mit histochemischen und elektrophysiologischen Methoden untersucht:

Färbungen mit der NADPH Diaphorase Technik, einem histochemischen Nachweisverfahren für NO Synthase, ergaben positive Resultate im reifen Riechepithel und eine auffallend dynamische Entwicklung des Färbemusters während des ersten Lebensmonats. Immunhistochemische Doppelmarkierungen mit einem Antikörper gegen ein Riechsinneszellen-spezifisches Protein (Olfactory Marker Protein) zeigten, dass es sich bei den NADPH Diaphorase-markierten Zellen um ausgewachsene Riechsinneszellen handelt. Diese Ergebnisse deuten darauf hin, dass eine NO-Quelle auch nach der Geburt im olfaktorischen Epithel vorhanden bleibt, und an der späten Entwicklung des Riechepithels beteiligt ist.

Die elektrophysiologischen Experimente ergaben, dass NO in der Riechsinneszelle einen hyperpolarisierenden Kaliumstrom auslöst. Dieser Effekt liess sich durch die Ionenkanal-Blocker Tetraethylammonium, Charybdotoxin und Iberiotoxin reduzieren oder eliminieren, was auf die Aktivierung von Kalzium-abhängigen Kaliumkanälen hinweist.

Mit Hilfe von Kalziumkanal-Blockern, Kalzium-Imaging und der direkten Messung von Kalziumströmen konnte gezeigt werden, dass NO einen Kalzium-Einstrom in die Riechsinneszelle auslöst, welcher dann die Kalzium-abhängigen Kaliumkanäle öffnet. Vergleichbare Ergebnisse aus *Caudiverbera*, *Xenopus* und der Ratte suggerieren eine generelle Eigenschaft von Wirbeltier Riechsinneszellen.

Schliesslich wurde demonstriert, dass NO auch die Riechtransduktionskanäle öffnen kann. Hohe NO-Konzentrationen aktivierten die Kanäle ohne die Hilfe von cAMP oder anderer Agonisten. cGMP war an dem Aktivierungsprozess nicht beteiligt, deshalb handelt es sich wahrscheinlich um eine direkte Modifikation des Kanalproteins durch NO. Da dieser Kanaltyp nicht nur in den Zilien, wo die Riechtransduktion stattfindet, sondern auch in den axonalen Wachstumskegeln der Rezeptorneurone vorhanden ist, könnte seine Stimulierung durch NO auf eine Funktion bei der Entwicklung der Riechsinneszellen hindeuten.

Stichworte zum Inhalt:

NO, Riechsinneszelle, NADPH Diaphorase

Abstract

The sensory neurons of the olfactory epithelium are continuously replaced during life. Every newly generated neuron has to extend a dendrite to the apical surface of the epithelium, grow cilia there and, above all, send an axon to a correct glomerulus of the olfactory bulb and establish synaptic connections.

It has been reported that nitric oxide (NO) synthase is transiently expressed during embryonic development and the bulbectomy-induced regeneration of olfactory receptor neurons, suggesting a function of NO within axonal outgrowth, pathfinding and synaptogenesis. The mechanism of action of NO and the question of whether it maintains a role in the normal mature olfactory epithelium remained, however, unresolved. In the present work, this issue has been addressed by histochemical and electrophysiological approaches:

Labeling with the NADPH diaphorase method, a histochemical marker for NO synthase, gave positive results in the mature epithelium and showed a conspicuous development of the staining pattern during the first postnatal month. Immunohistochemical double-labeling with an antibody against olfactory marker protein confirmed the identity of the NADPH diaphorase-positive cells as mature olfactory receptor neurons. These results support the notion that a source of NO remains present in the olfactory epithelium after birth and is involved in the late development of the olfactory epithelium.

The electrophysiological experiments showed that NO activates a potassium current in the cell membrane, which leads to hyperpolarization of the cell. The effect is sensitive to the ion channel blockers tetraethylammonium, charybdotoxin and iberiotoxin, suggesting that the observed current is produced by the opening of calcium-activated potassium channels. The use of calcium channel blockers, calcium imaging and the direct measurement of calcium currents indicated that NO causes a calcium influx into the olfactory receptor neuron, which in turn activates the calcium-dependent potassium channels.

Comparable results were observed in *Caudiverbera*, *Xenopus* and the rat, suggesting that they represent a general feature of vertebrate olfactory receptor neurons.

Finally, NO was shown to activate the cyclic nucleotide-gated transduction conductance in whole-cell patch clamp experiments. High concentrations of NO opened the transduction conductance without the presence of cyclic AMP or other agonists. This effect was insensitive to the soluble guanylyl cyclase-inhibitor ODQ and hence independent from cyclic GMP, therefore it is most likely a direct action of NO on the channel protein. As these channels are not only present in the olfactory cilia, where transduction occurs, but also in axonal growth cones, the data are consistent with the idea that NO is involved in the development of olfactory receptor neurons.

Key words:

Nitric oxide, olfactory receptor neuron, NADPH diaphorase

Parts of this thesis have been published in the following research articles:

1. Oliver Schmachtenberg and Juan Bacigalupo. 1999. Nitric Oxide Activates a Potassium Current in Olfactory Receptor Neurons from *C. caudiverbera* and *X. laevis*.
   Brain Res **837,** 301-305

2. Oliver Schmachtenberg and Juan Bacigalupo. 2000. Calcium Mediates the NO-induced Potassium Current in Toad and Rat Olfactory Receptor Neurons.
   J Mem Biol **175,** 139-147

3. Oliver Schmachtenberg, Gerd Bicker and Juan Bacigalupo. 2001. NADPH diaphorase is developmentally regulated in rat olfactory epithelium.
   NeuroReport **12**(5):1039-43

Abbreviation	Full name
cAMP	adenosine 3',5'-cyclic monophosphate, a second messenger
cGMP	guanosine 3',5'-cyclic monophosphate, a second messenger
CNG channel	cyclic nucleotide-gated channel, e.g. the olfactory transduction channel
ChTX	charybdotoxin, potent selective potassium channel blocker
DPIP	dichloroindophenol (also DCIP), a flavoprotein and NOS inhibitor
GTP	guanosine 5'-triphosphate, a precursor of cGMP
FITC	fluorescein isothiocyanate
Hb	hemoglobin, NO scavenger
IbTX	iberiotoxin, a potent selective blocker of Ca^{2+}-dependent K^{+}-channels
I-clamp	current-clamp
K_{Ca}-channel	calcium-dependent potassium channel
LY83583	blocker of the olfactory CNG channel and an inhibitor of sGC
NADPHd	nicotinamide adenine dinucleotide phosphate diaphorase
NO	nitric oxide
NOC-12	3-ethyl-3-(ethylaminoethyl)-1-hydroxy-2-oxo-1-triazene, NO-donor
NOS	NO synthase
ODQ	oxadiazolo[4,3a]quinoxalin-1-one, a potent inhibitor of sGC
ORN	olfactory receptor neuron
P0, P1 etc.	postnatal day 0 (day of birth), etc.
PBS	phosphate-buffered saline
SD	standard deviation
SEM	standard error of median
sGC	soluble guanylyl cyclase, a principal target of NO
IS	intracellular solution
SNAP	S-nitroso-N-acetylpenicillamine, NO-donor
SNP	sodium nitroprusside, NO donor

1. Introduction

1.1. General properties of nitric oxide (NO)

NO is a free radical gas. It is small, reactive and membrane-permeable. In biological systems, it is synthesized by the three isoforms of the enzyme NO-synthase (NOS), each of which performs very different functions in the animal organism: *1.* Endothelial NOS produces NO as the formerly known endothelium-derived relaxation factor (EDRF) to regulate vascular smooth muscle tone and blood pressure. *2.* Inducible NOS, which is found in cells of the immune system, synthesizes NO as a cytotoxic agent to fight bacteria and parasites, and *3.* neuronal NOS generates the molecule as a neuronal messenger in the nervous system.

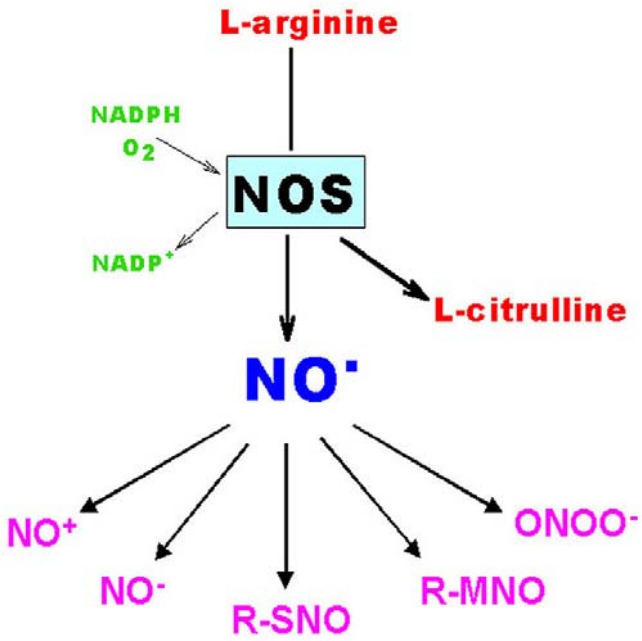

Fig. 1. NO-chemisty
NO, produced by NO-synthase from L-arginine, may convert to or be enzymatically transformed into NO^+, NO^- and $ONOO^-$ (peroxynitrite), all of which have biological functions as well. Interactions with proteins occur principally through S-nitrosylation of cysteine-residues or transition metals, yielding nitrosothiol (R-SNO) and metal nitrosyl (R-MNO) groups.

All NOS isoforms catalyze NO from L-arginine with molecular oxygen and NADPH as co-factors; co-product is L-citrulline [Marletta, 1994; Fig. 1]. However, whereas inducible NOS produces NO continuously, both endothelial and neuronal NOS are regulated by intracellular calcium through the bound co-factor calmodulin. In neurons, liberation of NO responds to calcium entry caused by activity-dependent depolarization. As the use of a small gaseous molecule for signaling in biological systems is a fairly new and unusual concept, the theories developed to describe its actions still require some imagination: From its source, NO may reach nearby inter- or intracellular targets by free diffusion within a sphere around its synthase. In this model, specificity is achieved by the (sub)cellular localization of both NOS and its target protein, and the field of action is limited by the short half-life, high reactivity and rapid spatial dilution of NO [see Garthwaite & Boulton, 1995]. Alternatively, NO may be channeled by protein-guided transport, which requires a specialized machinery, but implies a longer lifetime and possibly higher local target concentrations [see Stamler et al., 1997].

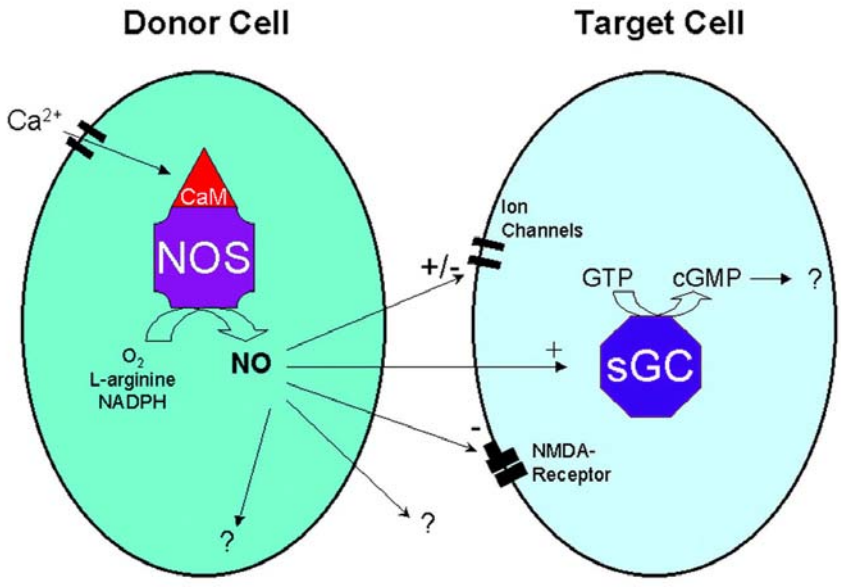

Fig. 2. NO-signaling
In neurons, NO-synthesis is regulated by intracellular calcium. Once liberated, NO diffuses to a neighboring cell and affects various ion channels or enzymes like soluble guanylyl cyclase (sGC), resulting in the elevation of cGMP-levels in the target cell. As an autocrine messenger, NO may also act on targets within its donor cell.

Among the variety of NO-targets that have been identified, the best-known and maybe most important one is the enzyme soluble guanylyl cyclase, which synthesizes the intracellular messenger cyclic GMP [cGMP; Bredt & Snyder, 1989]. NO binds reversibly to the prosthetic heme group of soluble guanylyl cyclase and activates the enzyme at nanomolar concentrations (Fig. 2). cGMP, in turn, acts on a large number of downstream targets including protein kinases, phosphodiesterases and ion channels.

Other important functions of NO make use of its capacity to readily attach covalently to protein-bound thiol residues and transition metals, resulting in local reactivity of these groups and conformational changes of the target protein. Notably the S-nitrosylation of cysteine residues has been established as a physiological action mechanism of endogenous NO [Jaffrey et al., 2001]. Examples of this generally termed “redox” signaling include the direct activation of certain potassium and calcium channels and the inhibition of the N-methyl-D-aspartate (NMDA) receptor in the nervous system [reviewed by Stamler et al., 1997; Barañano et al., 2001].

1.2. The olfactory epithelium

The olfactory epithelium is the smelling sense organ of vertebrates. Its functional units, the olfactory receptor neurons, localize with their cell bodies to the central zone of the epithelium. Their axons traverse the basal lamina and terminate in a glomerulus of the olfactory bulb of the brain, where they form synapses with mitral cell dendrites. From the soma of the olfactory receptor neuron, a single dendrite projects to the epithelial surface, where a bundle of cilia originates from its terminal, called olfactory knob (Fig. 3). The cilia are the organelles of olfactory transduction, containing the G-protein-coupled seven transmembrane odor receptors. Each olfactory receptor neuron is thought to express receptor proteins of just one type [Malnic et al., 1999]. Binding of an odor molecule to a receptor activates an enzymatic transduction cascade, which results in the elevation of cyclic AMP (cAMP) levels in the

cilium. cAMP directly opens the cyclic nucleotide-gated channels, through which sodium and calcium enter the cilia. Intracellular calcium in turn directly activates the ciliary calcium-dependent chloride channels, thus amplifying the transduction current. The resulting depolarization of the neuron raises the frequency of action potentials that convey the signal to the olfactory bulb. Inhibitory odor responses are also observed, but are not yet completely understood [Sanhueza et al., 2000; see Schild & Restrepo, 1998].

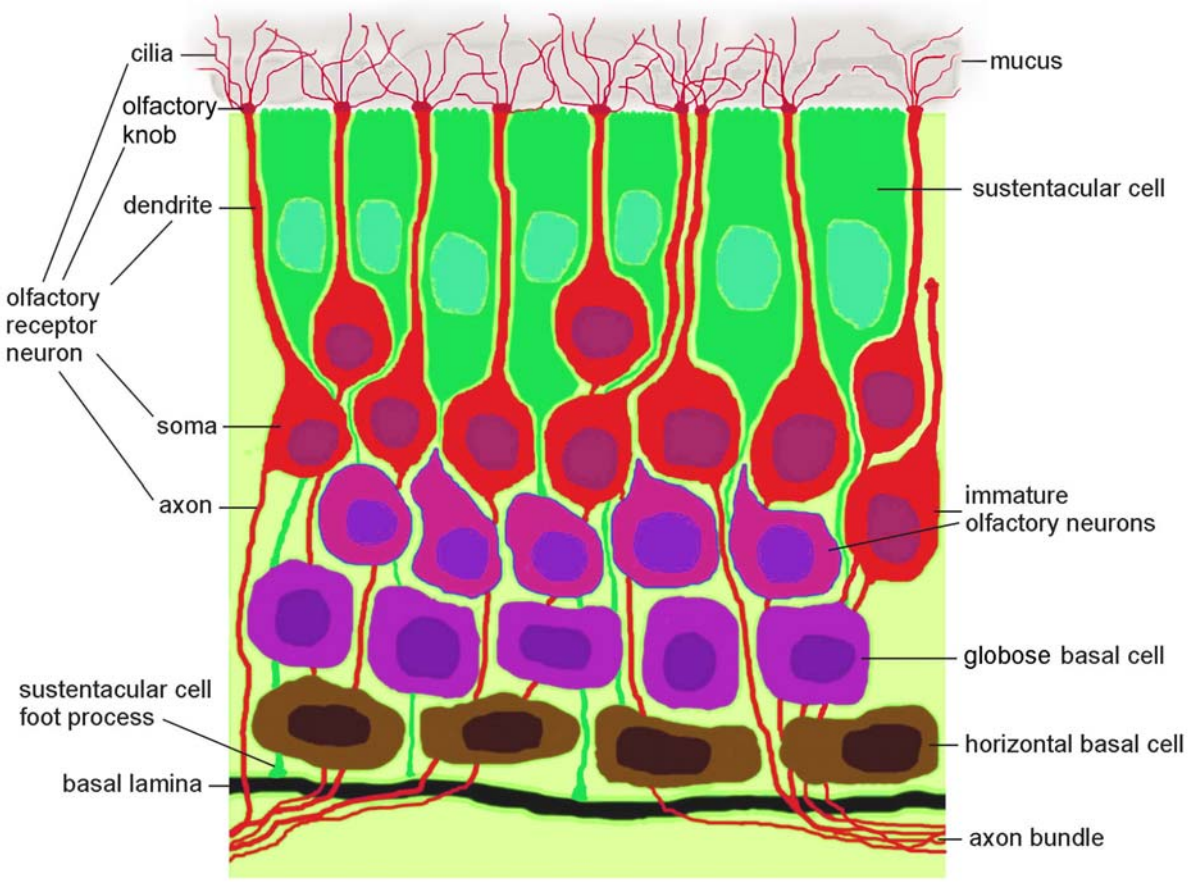

Fig. 3. Schematic view of the olfactory epithelium
The olfactory epithelium consists of three principal cell groups: Sustentacular cells, olfactory receptor neurons and basal cells (the cells of the Bowman glands are not shown). According to the lineage system of the olfactory epithelium, which has recently been established [Huard et al., 1998], the multipotent globose basal cells are the neuronal progenitors, but may also produce the other cell types in the case of severe epithelial damage.

Although protected by the outer layer of sustentacular cells, the olfactory receptor neurons are exposed to noxious stimuli and frequent mucosal infections and must therefore be replaced continuously during the lifetime of the animal. Together with the hippocampus and the olfactory bulb, this represents one of the few known examples of regular neuronal replacement the nervous system and a great developmental challenge for the organism, because each new axon has to find its way to the correct one (or few) of many glomeruli in the olfactory bulb, where signals from all olfactory neurons with the same odor receptor molecule converge.

1.3. NO in the olfactory epithelium

In the olfactory epithelium, NO has been implicated in three different physiological complexes: *1*. odor transduction, *2*. perireceptor processes and *3*. neuronal development.

Regarding odor transduction, a stimulation of soluble guanylyl cyclase by NO has been reported for ciliary preparations of rat olfactory receptor neurons, where odorant-induced rises of cGMP levels could be abolished by the NOS-inhibitor l-nitroarginine and the NO-scavenger hemoglobin [Breer et al., 1992], suggesting the odor-induced synthesis of NO and an alternative olfactory transduction pathway in these cells.

Lischka & Schild [1993] found induction of inward currents by the NO-donor sodium nitroprusside (SNP) in voltage-clamped isolated *Xenopus* olfactory receptor neurons. As these currents were similar to those elicited by cGMP, the authors proposed a NO/cGMP-system in olfactory receptor neurons. More recently, comparable results have been obtained in the turtle [Inamura et al., 1998]. On the other hand, a direct, cGMP-independent activation of the olfactory cyclic nucleotide-gated channels by NO has been described for salamander olfactory receptor neurons and proposed for the rat [Broillet & Firestein, 1996[a]; 1996[b]]. In this case, NO covalently attaches to a cysteine residue of the channel protein, leading to a conformational change that favors the open state [Broillet, 2000].

Whether NO actually participates in olfactory transduction remains nonetheless unclear, because effects of NO on olfaction have never been shown *in vivo*, and because the temporal expression pattern of NOS within the olfactory receptor neurons is still a matter of discussion. Although some biochemical assays suggest a constitutive expression of NOS in the olfactory epithelium [Breer & Shepherd, 1993; Dellacorte et al., 1995], several laboratories have unsuccessfully tried to show the presence of NOS in mature olfactory receptor neurons with immunohistochemical methods [Kishimoto et al., 1993; Bredt & Snyder, 1994]. Yet, this negative result might possibly be explained by the presence of a splicing variant of NOS [Eliasson et al., 1997] that is not recognized by common NOS antibodies.

As opposed to the controversial NOS-expression in olfactory receptor neurons, it has been clearly established that neuronal NOS is present in the perivascular autonomous nerve terminals which innervate the blood vessels and submucosal glands of the olfactory epithelium [Hanazawa et al., 1994; Kulkarni et al., 1994; Lee et al., 1995]. By regulating local epithelial blood flow NO might indirectly influence olfactory processes, but a direct effect on olfactory receptor neurons appears unlikely due to the great distance of that NO source from the olfactory receptor neuron somata and dendrites.

Finally, neuronal NOS has been shown to be transitorily expressed within olfactory receptor neurons during the embryonic and early postnatal development of the rat [Roskams et al., 1994; Bredt & Snyder, 1994]. These histological data led to the hypothesis of NO-signaling during developmental processes like axonal and dendritic outgrowth and suggested a role for NO within the establishment of synaptic connections in the olfactory bulb. Similar results have been obtained from mouse embryos with a slightly different time course of NOS expression, and here, the inducible NOS isoform was detected instead of neuronal NOS [Arnhold et al., 1997].

However, physiological data about this putative NO-signaling during embryonic development are missing, and the question whether NO continues to be involved in the

comparable processes of neuronal regeneration within the mature olfactory epithelium remains to be resolved.

1.4. Hypothesis, methodological approach and objective

The diverse studies regarding NO and olfaction that have been published during the last eight years leave an incoherent, puzzling image. Nonetheless, they altogether suggest that NO has important functions in the olfactory epithelium.

This doctoral thesis is based on the hypothesis that NO is involved in the developmental processes of the olfactory epithelium. These comprise the embryonic and postnatal development and the continuous regeneration that occurs within the mature olfactory epithelium. The possibility that NO plays a role in the physiology of olfactory transduction and adaptation is also considered.

To investigate this theme, a combination of histological and electrophysiological approaches has been chosen to gather information concerning two basic issues of putative NO-signaling in the olfactory epithelium: *1.* Where and when is NOS expressed? and *2.* how does NO affect olfactory receptor neurons?

Accordingly, the objective was to describe the temporo-spatial expression pattern of NOS in the olfactory epithelium with histological methods and to analyze the immediate physiological effects of NO on isolated olfactory receptor neurons with the patch clamp technique.

2. Materials and Methods

2.1. Animals

Wistar rats were either bred in the laboratory or bought from the animal facility of the Catholic University of Chile. The toad *Caudiverbera caudiverbera* was caught in the south of Chile and held in the animal house of the laboratory. *Xenopus laevis* was bred in the laboratory.

Caudiverbera olfactory receptor neurons (ORNs) are especially suitable for patch clamp experiments due to their big size (soma diameter ≈ 15 μm) and the fact that healthy cells can be readily recognized by their beating cilia, therefore they were initially used as electrophysiological model system. On the other hand, the facts that the toads cannot be bred in the laboratory and that they are relatively unknown in the international scientific community represent certain disadvantages. For that reason, *Caudiverbera* was later replaced by *Xenopus* and the rat.

2.2. Solutions

Phosphate-buffered saline (PBS, g/l):

8 NaCl, 0.2 KCl, 1.44 Na_2HPO_4, 0.24 KH_2PO_4, pH 7.4

Fixer: 4% paraformaldehyde in PBS, pH 7.4

Amphibian Ringer (mM): 110 NaCl, 2.5 KCl, 1 $CaCl_2$, 1.5 $MgCl_2$, 10 HEPES, 3 glucose, pH 7.6. Low Ca^{2+}-Ringer contained 0.1 mM $CaCl_2$.

Mammalian Ringer (mM):

130 NaCl, 4 KCl, 1.5 $CaCl_2$, 0.5 $MgCl_2$, 0.5 $MgSO_4$, 5 HEPES, 15 glucose, pH 7.4.

Intracellular solution (mM): 120 KCl, 1 $MgCl_2$, 1 $CaCl_2$, 2 EGTA, 4 HEPES, 0.1 GTP, 1 ATP, 13 sucrose, pCa 8.0, pH 7.6.

To measure Ca^{2+} currents, the intracellular solution contained (mM):

110 Cs methanesulfonate, 10 CsFl, 15 CsCl, 5 Cs-Hepes, 4 Mg-ATP, 10 phosphocreatin, pH 7.5, and the bath solution was supplemented with 10 mM TEA.

2.3. Preparation of frozen sections of the olfactory epithelium of the rat

Rats were sacrificed by CO_2-inhalation for 2-3 min, decapitated and the nasal cavity was opened by a transversal section of the skull. The olfactory epithelium, which covers the dorsal posterior part of the nasal septum and the adjacent bony structures called turbinates, was excised with fine scissors. As no difference could be observed between olfactory epithelium from the septum and the turbinates, it was later taken exclusively from the septum. The tissue was fixed in a freshly prepared solution of 4% paraformaldehyde (pH 7.4) at 4°C for 1 h or over night, and stored for 24 h in a solution of 30% sucrose in phosphate-buffered saline (PBS) at 4°C for cryoprotection. Hereafter, the epithelium was blotted dry, embedded in tissue freezing medium (*TBS*) and frozen at -20°C in a cryostat (*American Optical*). Coronal sections of 20 µm thickness were cut at -20°C, placed on microscope slides covered with Pegotin (*BiosChile*) for adherence, air-dried and stored at 4°C for up to 48 h.

2.4. NADPH diaphorase (NADPHd) staining of cryosections

The NADPHd staining solution was prepared by dissolving 1 mg/ml nitro blue tetrazolium in methanol, diluting this to 0.1 mg/ml in PBS and adding reduced β-nicotinamide adenine dinucleotide phospate (β-NADPH) to a final concentration of 0.1 mg/ml.

After rehydration of the sections in PBS with 0.1% Triton X-100, the NADPHd reaction was started by the addition of the NADPHd staining solution. The reaction was continued at room temperature for 2 h or until the color saturation was satisfactory, and terminated by rinsing in PBS. As a control, the flavoprotein inhibitor 2,6-dichloroindophenol

(DPIP) was added at a concentration of 100 μM to some of the preparations. After the staining procedure, the cryosections were rinsed in distilled water and stored in glycerol at 4°C. Microphotographs were taken with a cooled CCD camera *(Spot Diagnostic Instruments*) attached to an *Olympus* BX-60 microscope.

2.5. NADPHd staining of dissociated olfactory receptor neurons

ORNs from the rat were dissociated as described in section 2.8. After having settled on the Pegotin-covered microscope slides for 20 min, the cells were fixed in 4% paraformaldehyde solution over night at 4°C. Finally, they were stained according to the protocol of section 2.4.

2.6. NADPHd – olfactory marker protein (OMP) double labeling

For OMP – NADPHd double labeling, sections were first NADPHd-stained, then blocked in 20% rabbit serum in PBS with 0.1% Triton X-100 for 30 min at room temperature and finally incubated at 4°C overnight in the primary OMP antiserum, a friendly gift from Dr. F.L. Margolis (University of Maryland), diluted 1:1000 in PBS with 0.1% Triton X-100. Sections were incubated in the secondary FITC-coupled rabbit anti-goat antibody diluted 1:200 in PBS for 2 h at room temperature, washed and stored in glycerol.

2.7. Cell counts

To count stained cells, photographs of the sections were contrast-enhanced with the computer program *Adobe Photoshop 4.0*. Cells were counted manually over defined lengths of olfactory epithelium, averaged (8 – 10 counts per preparation) and normalized to 1 mm of epithelial length.

2.8. Preparation of dissociated olfactory receptor neurons

ORNs were isolated from *C. caudiverbera*, *X. laevis* and the rat.

The amphibians were cooled down to 0°C for insensibilisation, sacrificed and pithed before opening the nose chamber. The olfactory epithelium was removed with fine scissors, cut into pieces of ~1 mm^2 and stored in amphibian Ringer supplemented with 1% bovine albumin at 4°C for up to 48 h.

The olfactory epithelium of the rat was excised as described in section 2.3. The epithelium was cut into small pieces of ~1 mm^2, stored in *Leibovitz* L-15 medium at 4°C and used only on the day of the preparation. Dissociation of the epithelia from all species was achieved by trituration through a fire-polished Pasteur pipette with an approximate tip diameter of 0.5 mm, without the use of enzymes. Cells were let settle for 20 min in the recording chamber coated with Pegotin (*BiosChile*) and washed with Ringer. A few control experiments without Pegotin produced identical results.

2.9. Patch clamp recordings

The patch clamp technique was used in its voltage clamp and current clamp modes [Hamill et al., 1981] to record the electrical activity of dissociated ORNs. Electrical recordings were obtained using a PC-501A amplifier (*Warner Inst.*) and pClamp 6.0 software (*Axon Instruments*). Recording pipettes were drawn from Blu Tip capillary tubes (*Oxford Labware*) in a horizontal Puller (*Sutter* P-97) to a tip resistance of 3 - 6 MΩ. Cells were observed with an inverted *Olympus* IX 70 microscope with attached video camera. Whole-cell mode was established by oral suction, capacity was compensated and signals were low pass filtered at 5 kHz. Only experiments with seal resistances > 1 GΩ (typical ≥ 4 GΩ) were considered. Between experiments, *Caudiverbera* and *Xenopus* ORNs were held at a resting membrane potential of –70 mV; rat ORNs at –80 mV.

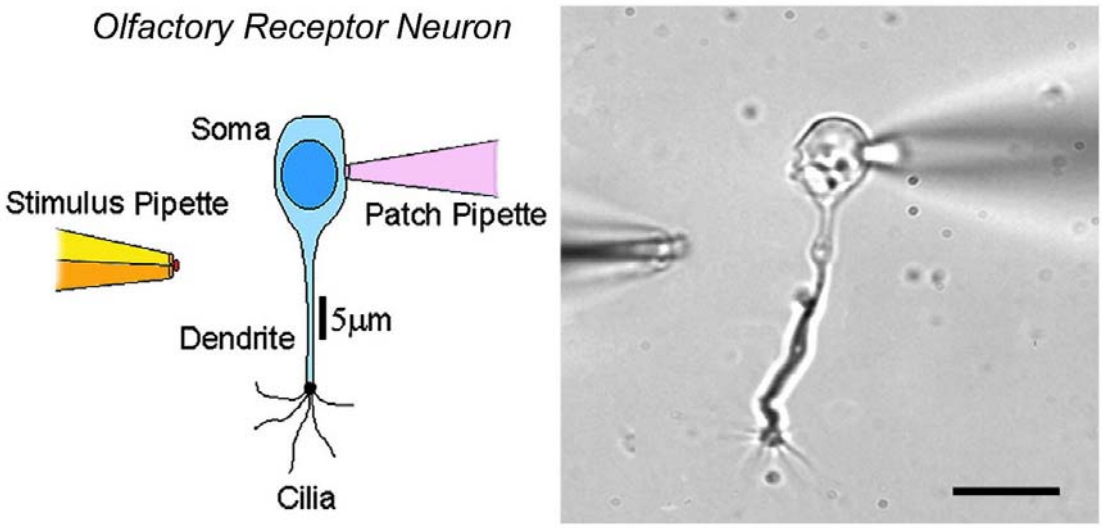

Fig. 4. Schematic view and photograph of the patch clamp technique applied. Stimulation was achieved with a triple-barreled stimulus pipette positioned towards the middle of the cell, the soma or the cilia, according to the experiment. The neuron on the right is from the rat (scale bar = 10 µm).

2.10. Stimulation

Pharmacological stimuli were generally applied focally to the patched cells by computer-controlled pressure ejection. In this case, pulses of varying duration (0.5 s – 1 min) and pressures (0.3 – 1.0 bar) were produced using a picospritzer and double- or triple-barreled glass pipettes (*Sutter*, tip diameter ca. 1.5 µm), positioned at a distance of 15 - 40 µm from the cell. Pressure ejection was monitored visually to verify that the stimulus pipette was not blocked. The stimulus concentrations reaching the cells were lower than the concentrations in the stimulus pipette because of dilution in the recording bath and due to the unstirred layer around the cell membrane. The dilution factor was estimated to be in the range between ~ 1 and 3. In a few cases, perfusion of the entire recording chamber was used to add a reactive or to change the ionic composition of the external solution.

Nitric oxide (NO) was applied with the use of NO-releasing compounds (NO-donors, 10 mM in Ringer), which liberate the gas in a time-dependent manner. Sodium nitroprusside

(SNP), used as standard NO-donor, was prepared freshly before the experiments and protected from light. Alternatively, NOC-12 and SNAP (*Calbiochem*) were used in some experiments. As additional controls, SNP was applied after its inactivation by ventilation under light for 48 h, and hemoglobin (Hb) was used as NO-scavenger at a concentration of 10 mg/ml.

In order to block potassium conductances, the ion channel blocker tetraethylammonium (TEA) was used at a concentration of 2 mM, charybdotoxin (ChTX) and iberiotoxin (IbTX; a gift from Dr. R. Latorre) at 200 nM and apamin (*RBI*) at 2 μM. To block calcium channels, cadmium chloride ($CdCl_2$) was applied at 100 μM and nifedipine at 50 μM. LY83583 (*RBI*) was used to block the cyclic nucleotide-gated transduction channels [Leinders-Zufall & Zufall, 1995] at 20 and 40 μM in the stimulus pipette. In the experiments with TEA, $CdCl_2$, nifedipine and low Ca^{2+}, the cells were microsuperfused using one of the stimulus pipette barrels. The second barrel contained the respective solution with 10 mM SNP and the third barrel SNP in normal Ringer. In other cases, drugs were coejected with SNP and compared with SNP- and drug-effects alone. For some experiments, SNP (10 mM) or cAMP (100 μM) were added directly to the intracellular solution.

To inhibit the NO-target soluble guanylyl cyclase, ODQ was either added to the stimulus pipette (1 μM or 100 μM) or to the intracellular solution (2 and 5 μM).

2.11. NO-measurements

The time course of NO liberation by 10 mM SNP dissolved in Ringer was measured with a *Sievers* NOA 280 nitric oxide analyzer (courtesy of M. Bóric and X. Figueroa) under conditions similar to those of the electrophysiological experiments (22-24°C, indirect dim neon light). The measured NO concentrations represent an approximation of the levels in the stimulus pipette and are therefore higher than the actual NO concentration reaching the cell with pulsed stimulation, estimated to be in the sub-micromolar range.

2.12. Calcium-imaging

Olfactory epithelium from *Caudiverbera* was loaded with 15 µM Fluo-3,AM (*Molecular Probes*) in 0.1% pluronic acid at 4°C for 30 min. After dissociation, cells were transferred to a Pegotin-coated coverslip. Images were obtained with a *Zeiss* Axiovert 135M confocal laser scanning microscope implemented with a 40x oil-immersion objective. SNP was applied with a picospritzer as in the electrophysiological experiments.

All chemicals were purchased from *Sigma*, unless otherwise indicated.

3. Results

PART A. HISTOCHEMICAL EXPERIMENTS

3.1. NADPHd is sensitive to the fixation conditions in the olfactory epithelium

NADPHd was used to detect the expression of NOS in the olfactory epithelium. Since this histochemical staining method is known to be sensitive to the fixation conditions [Matsumoto et al., 1993], these conditions have been varied initially in order to be optimized.

Fixation with 4% formaldehyde solution produced identical staining results as fixation in 4% paraformaldehyde solution (not shown), but the latter yielded better tissue preservation and was consequently used as general fixative. Fixation at room temperature diminished the staining intensity compared to fixation at 4°C, and was therefore discarded. The most important finding was, however, the strong dependence of the staining pattern on the fixation time. Fixation for 18 h in 4% paraformaldehyde at 4°C resulted in the purple labeling of a broad band of cells in the center of the olfactory epithelium of an adult rat (Fig. 5A). The outermost layer of the sustentacular cells and olfactory receptor neuron dendrites displayed a weaker staining, but no color reaction could be observed in the layer of the basal cells and in the area proximal to the basal lamina.

In turn, fixation for only 1 h in otherwise identical conditions yielded an intense blue labeling of the sustentacular cells, the Bowman glands and the submucosal glands (Fig. 5C). The layer of the olfactory receptor neurons was marked in a fainter purple. With longer fixation, this staining pattern, which has been reported previously [Zhao et al., 1994] converted progressively into the one displayed in Fig. 5A. Since the specificity of NADPHd as a NOS marker is based on its resistance against formaldehyde fixation [Matsumoto et al., 1993], only this persistent NADPHd reaction might possibly represent NOS.

As a control, the NADPHd reaction was performed in the presence of the flavoprotein inhibitor DPIP, which has been used to eliminate NOS-dependent NADPHd labeling in the

olfactory bulb, thereby differentiating it from the NOS-independent staining that is also observed in the glomeruli of this tissue [Spessert et al., 1994]. In the olfactory epithelium, DPIP prevented all staining under both fixation conditions (Figs. 5B, D), supporting the possibility that NADPHd corresponds to NOS.

3.2. NADPHd marks olfactory receptor neurons

Olfactory marker protein (OMP) is a cytosolic protein of unknown function that is principally and abundantly expressed in mature olfactory receptor neurons [Margolis, 1985], and therefore serves as a marker for this cell group. To characterize the population of NADPHd-positive neurons, double labelings of olfactory epithelium with NADPHd and anti-OMP immunohistochemistry were prepared from neonatal and adult rats.

At P1, both NADPHd and anti-OMP marked a fraction of cells from the upper middle zone of the epithelium (Fig. 6A). NADPHd stained essentially the somata, and only a few dendrites appear also colored. A blood vessel (bv) is stained due to the NOS-expressing extrinsic innervation mentioned in section 1.3. Anti-OMP histochemistry, in turn, marked somata, dendrites, olfactory knobs and axons, which form bundles proximal to the basal lamina. Although both markers stained neurons from the same cellular layer, co-localization within individual cells was rare, suggesting an independent expression of NADPHd and OMP.

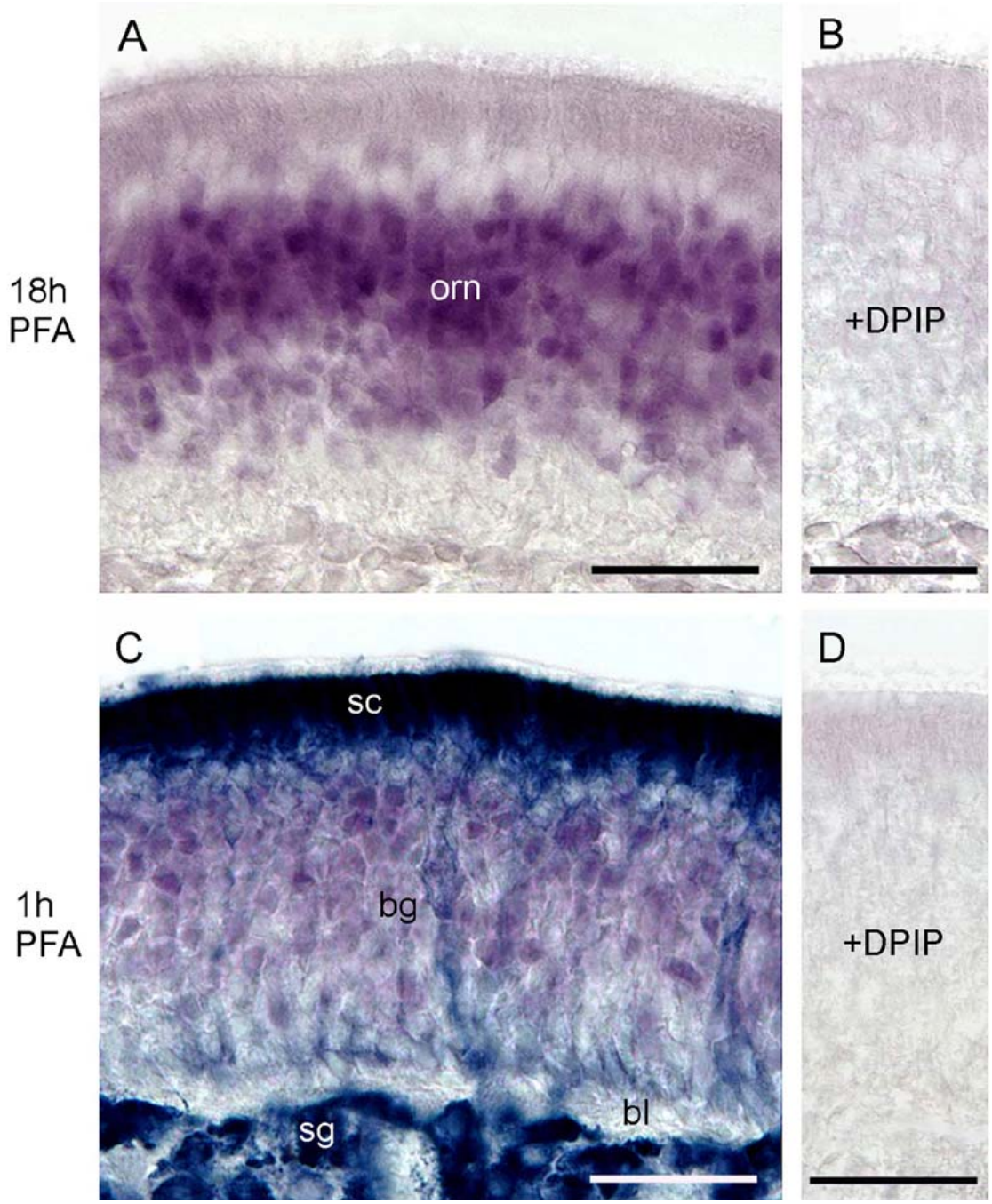

Fig. 5. NADPHd stainings of coronal sections through rat olfactory epithelium. The epithelial surface is up. **A**) NADPHd-staining of the olfactory epithelium of an adult rat after 18 hours of paraformaldehyde (PFA) fixation. Only cells in the layer of the olfactory receptor neurons (orn) are labeled. **B**) Addition of the flavoprotein inhibitor DPIP (100 µM) abolished all staining. **C**) A piece from the same epithelium, fixed for 1 hour only, yields a different staining pattern. Sustentacular cells (sc), Bowman glands (bg) and the submucosal glands (sg) proximal to the basal lamina (bl) display a dark-blue color as opposed to the light purple of the olfactory receptor neurons. To avoid color saturation, the NADPHd reaction had been stopped after 30 min. **D**) Addition of DPIP to the latter preparation prevented all staining. Scale bars = 50 µm.

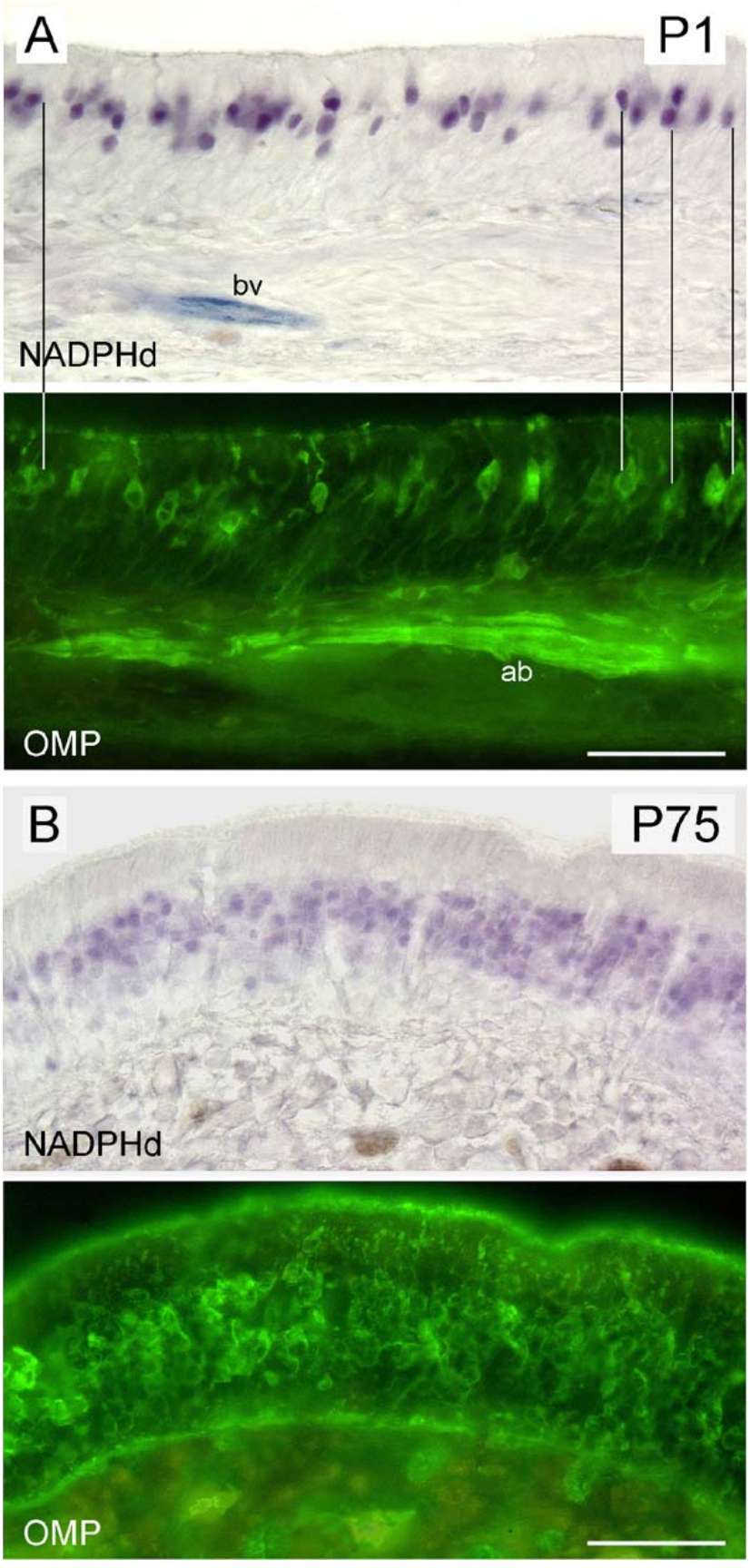

Fig. 6. NADPHd-OMP double labeling of the olfactory epithelium. **A**) At P1, a single layer of neurons is marked by both NADPHd and OMP immunohistochemisty, but co-localization within individual olfactory receptor neurons, as determined by computerized superposition, is found in only four cells (lines). OMP-positive axon bundles (ab) display no NADPHd reaction. NADPHd-positive nerve endings around a blood vessel (bv) are OMP-negative. **B**) At P75, both NADPHd and OMP are expressed in the broad central zone of the olfactory epithelium, where the cell bodies of the mature receptor neurons reside. The dendritic and ciliary layers are OMP-positive but NADPHd-negative. Scale bars = 50µm.

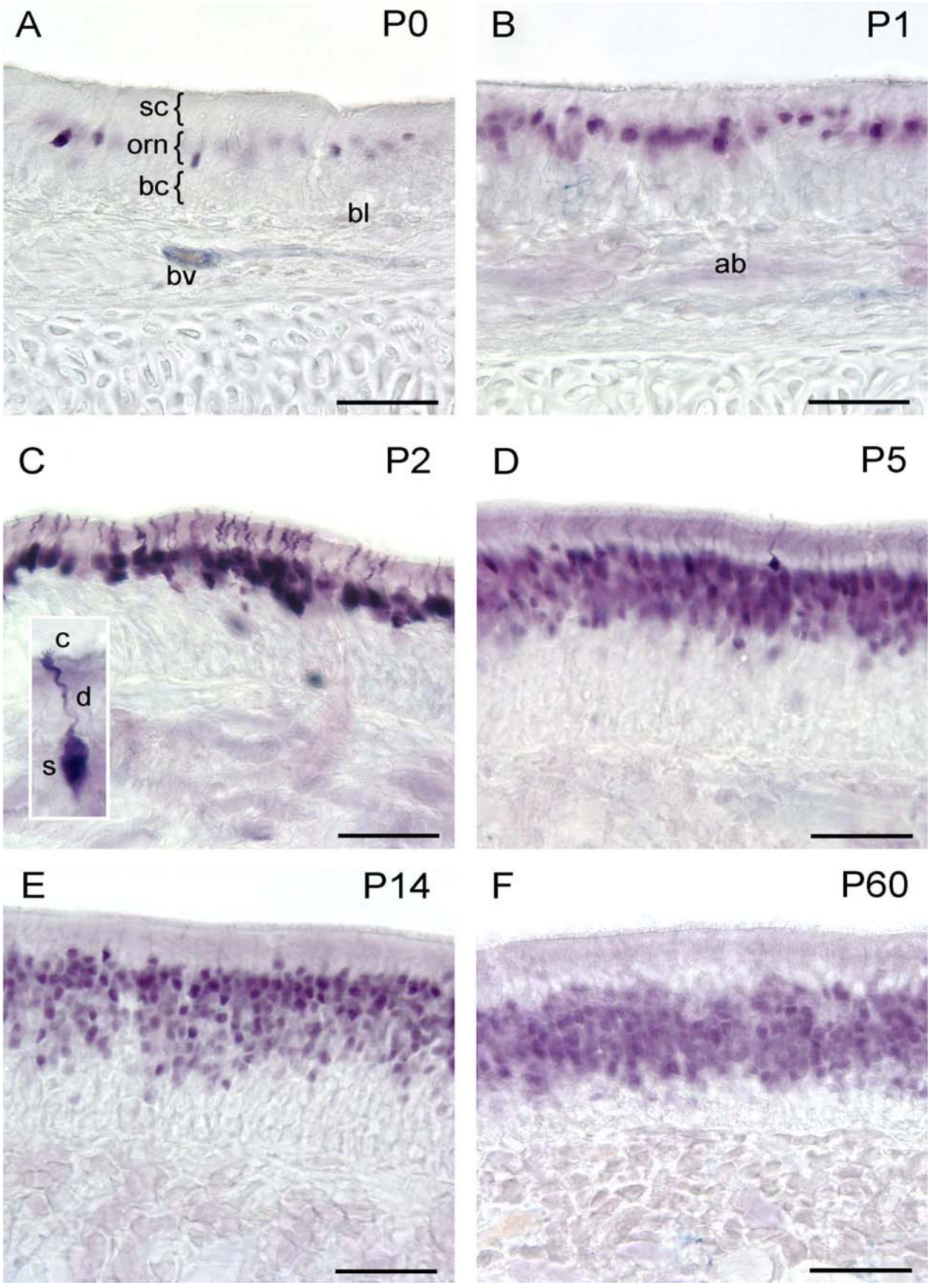
A
P0
sc
orn
bc
bl
bv
B
P1
ab
C
P2
c
d
s
D
P5
E
P14
F
P60

Fig. 7. (Anterior page). The NADPHd expression pattern changes during postnatal development. **A**) In newborn rats, only a few cell bodies in the olfactory receptor neuron (orn) layer are stained. No staining is seen among sustentacular cells (sc) and basal cells (bc). A blood vessel (bv) below the basal lamina (bl) is NADPHd-positive due to NOS-containing innervation. **B**) At P1, the NADPHd-positive cells have tripled. Dendrites, olfactory knobs and cilia remain unstained, but axon bundles (ab) are lightly stained. **C**) At P2, A densely packed row of NADPHd-positive somata (s) lines the outer third of the epithelium. Stained dendrites (d) project to the surface, where olfactory knobs and cilia (c) are labeled (see enlarged neuron in inset). **D**) At P5, three layers of stained somata form a 40 μm band in the external half of the epithelium. The outermost zone is densely packed with labeled dendrites, which display a reduced staining intensity. **E**,**F**) At later stages, the area of stained neurons broadens further, but many cells display a weaker staining, and the dendritic layer does not stain. P8 and P24 displayed no major changes and are not shown. Scale bars = 50 μm.

In the adult rat, the same broad band of cell bodies in the center of the olfactory epithelium was labeled by both markers (Fig. 6B). The abundant staining suggests considerable co-localization, but complicates a resolution at the single-cell level. Compared to the neonatal rat, the NADPHd labeling appears fainter.

3.3. NADPHd activity changes during postnatal development

To explore the developmental differences of NADPHd activity, preparations of olfactory epithelium from several developmental stages between P0 and P60 were stained and compared (Fig. 7). NADPHd was expressed in a small subset of olfactory receptor neurons as early as P0. After P0, the number of NADPHd-positive neurons increased rapidly, forming one almost continuous band of cells at P1, three bands at P5 and 5-6 at later stages. Whereas the NADPHd reaction generally predominated in the neuronal somata and especially in the nuclear and perinuclear region, a strong transitory NADPHd expression could be observed in the dendrites and olfactory knobs between P2 and P5. During this period, even the olfactory cilia were stained in some preparations (see inset in Fig. 7C). After P5, the staining in the dendritic layer diminished significantly, and the overall staining intensity also decreased with age.

The NADPHd-positive cells were further examined by applying the staining protocol to a preparation of dissociated olfactory epithelium from a rat at P3, which corresponds approximately to the peak of NADPHd intensity. A subset of isolated olfactory receptor neurons displayed strong staining of the soma, dendrite and olfactory knob (Fig. 8). Within the soma, the darkest color precipitate could be observed in the perinuclear region, suggesting that the NADPHd reactivity localizes to the nuclear membrane and the endoplasmic reticulum. No obvious differences in morphology were seen between stained and unstained neurons.

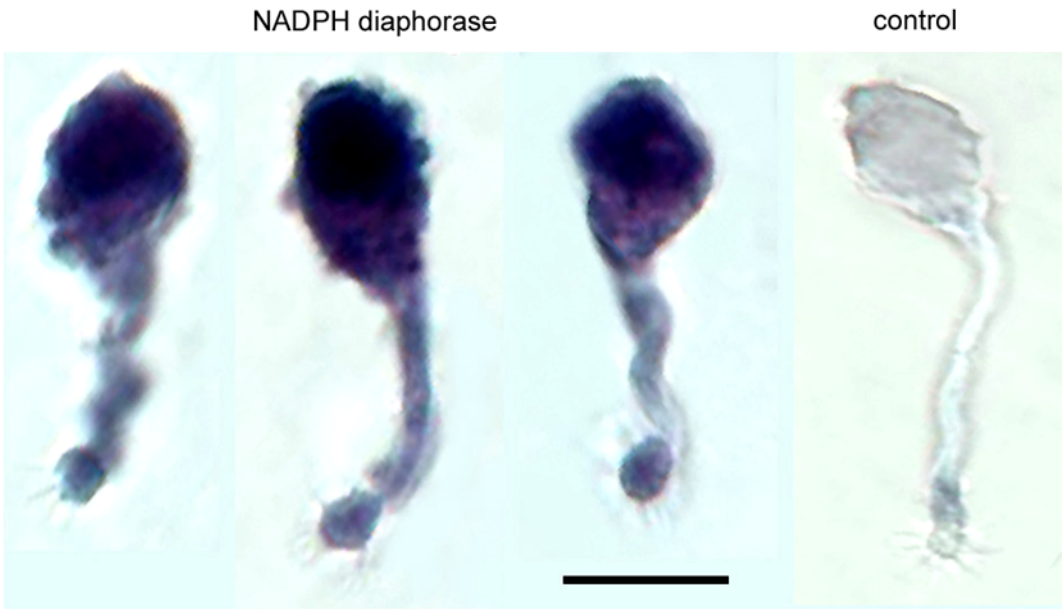

Fig. 8. NADPHd staining of dissociated olfactory receptor neurons from a P3 rat. The image shows three representative NADPHd-positive cells which display intense labeling of soma, dendrite and olfactory knob. Within the soma, the darkest staining is seen in the nuclear and perinuclear region. An unstained cell from the same plate is shown as control. Scale bar = 10 μm.

In order to quantify the relative number of NADPHd-positive neurons during postnatal development, these were counted over a defined length of olfactory epithelium from all analyzed stages (Fig. 9). The resulting graph shows a steep, more than tenfold increase of stained cells during the first month after birth. Hereafter, the number of NADPHd-positive neurons remains constant within the margins of error.

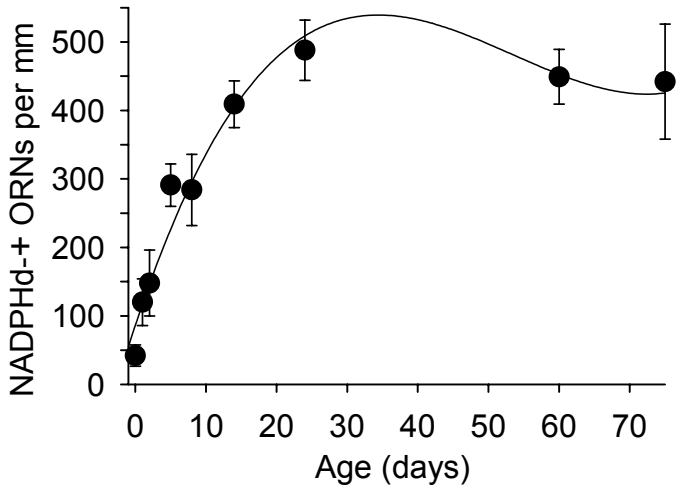

Fig. 9. The number of NADPHd-positive olfactory receptor neurons (ORNs) per unit length of 1 mm epithelium, plotted against the age. A tenfold increase of marked neurons is observed during the first two weeks, leading to a plateau after one month. Data represent the mean ± SD of 10 counts. The solid line is a third-order regression.

PART B. ELECTROPHYSIOLOGICAL EXPERIMENTS

3.4. Stimulation with NO

NO was applied to the patch clamped olfactory receptor neurons using pressure ejection of NO-donors. To find out if the applied doses were in a physiological range, the NO concentration produced by 10 mM SNP was measured with a nitric oxide analyzer. After dissolving SNP in Ringer, the NO concentration quickly rose to ~1 µM and remained relatively constant for at least 45 min (Fig. 10), which corresponds to the typical usage time of a stimulus pipette. 1 µM is considered a peak value at an endogenous NO source and is 1,000 times higher than an estimated biologically relevant threshold value [see Garthwaite & Boulton, 1995].

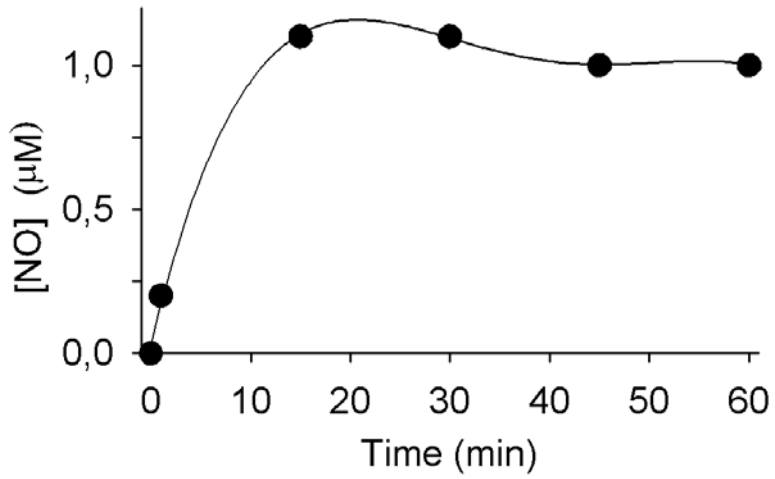

Fig. 10. Time course of NO-liberation by 10 mM SNP. The NO-donor was dissolved in Ringer at t = 0 min. The curve represents a 4^{th} order regression.

3.5. NO induces a hyperpolarizing potassium current in Caudiverbera olfactory neurons

Upon stimulation with pulses of NO-donors, current-clamped olfactory receptor neurons from *C. caudiverbera* (Fig. 11A) displayed a transient hyperpolarization of the membrane potential.

If the cells were discharging action potentials spontaneously, as is frequently the case, NO reduced the spiking frequency or abolished the activity transitorily (Fig. 11B).

In order to analyze the currents underlying this hyperpolarization, the experimental mode was changed to voltage clamp. Here, large outward currents were observed at depolarized membrane potentials upon NO-stimulation (Fig. 11C). A total of 98 out of 125 (78%) olfactory receptor neurons from *Caudiverbera* displayed this effect. The outward current developed with a short delay of ≥ 30 ms after the stimulus onset and returned to control levels 2 – 5 s after its end. In voltage ramp experiments, NO induced an outward current over the whole voltage range tested (Fig. 11D). The current becomes evident at –40 mV, peaks at +40 mV and generally declines towards +60 mV.

To assure that the effect was actually caused by NO and not by the NO donor molecule, the NO-scavenger hemoglobin was added to the stimulus solution. As shown in Fig. 12A, hemoglobin largely abolished the outward current. Further evidence for NO as inductor of the observed effect was obtained by the use of inactivated SNP, that did not produce any currents (Fig. 11C), and with NOC-12, an alternative but equally effective NO-donor with a molecular structure completely different from SNP (Fig. 15, n = 4).

As one of the principal functions of NO is the activation of the enzyme soluble guanylyl cyclase (sGC), the above experiments were repeated in different cells in the presence of the sGC-inhibitor ODQ and without the cGMP precursor guanosine triphosphate (GTP) in the intracellular solution (Fig. 12B). However, the NO-induced current was observed unchanged under these conditions, discarding the possibility that NO was acting via an elevation of cGMP levels.

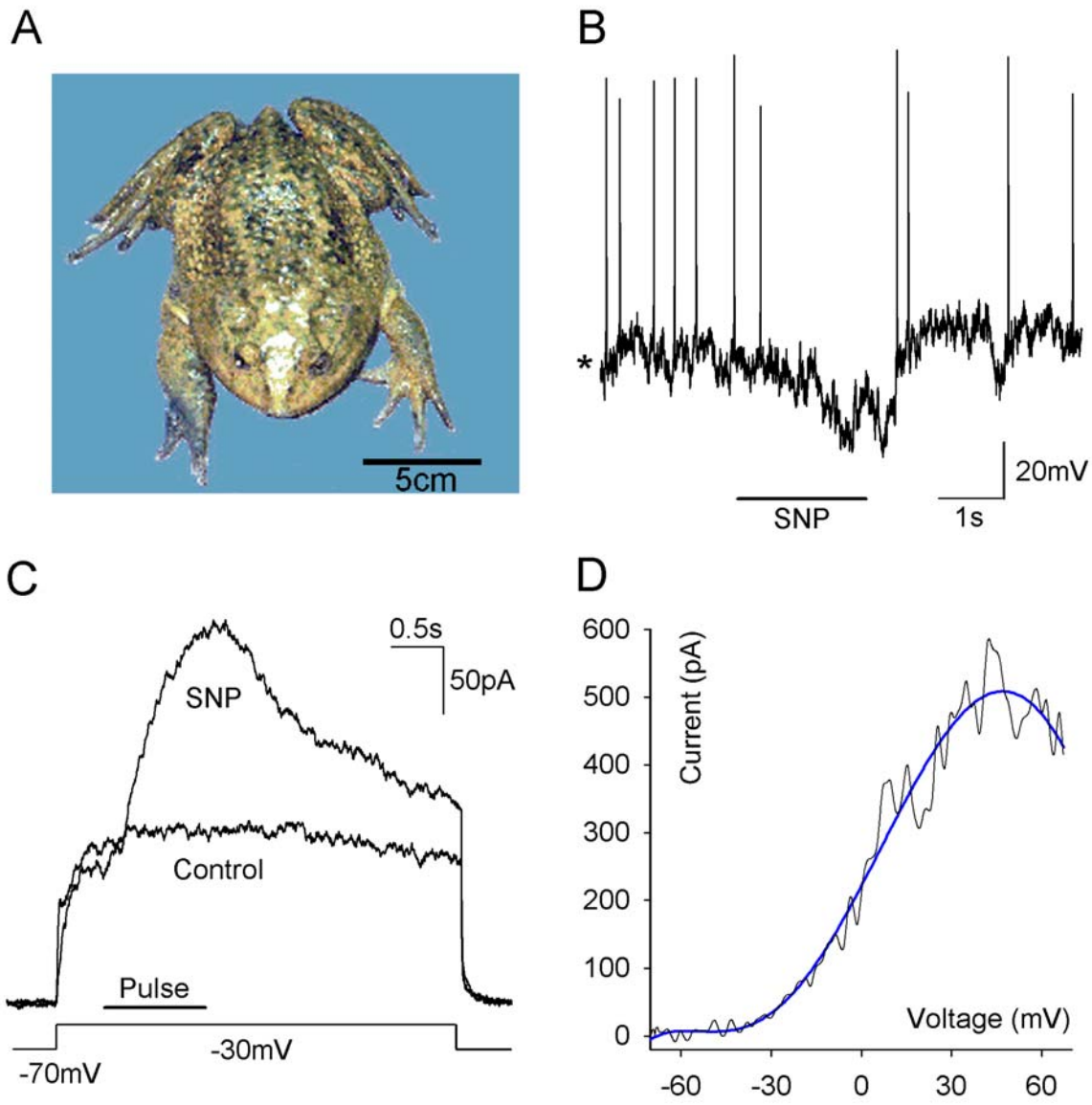

Fig. 11. NO causes a hyperpolarizing potassium current in *Caudiverbera* olfactory receptor neurons. **A**) The Chilean toad *C. caudiverbera* was initially chosen as model system to obtain dissociated olfactory receptor neurons. **B**) The NO-donor SNP (10 mM in the stimulus pipette) induced a transient hyperpolarization of the membrane potential in the neurons under current-clamp (n = 4). Resting membrane potential –55 mV (*). **C**) A pulse of SNP, applied during a voltage step from –70 to –30 mV, caused a rapid transient outward current under voltage-clamp (n = 98). In the control experiment, the cell was stimulated with inactivated SNP (n = 5). The control current results from the activation of voltage-gated channels by the depolarization to –30 mV. **D**) The current-voltage relationship of the SNP-effect from (C), obtained with a voltage ramp (-70 to +70 mV, 250 ms duration) applied at the peak of the current. A control current (induced by a ramp during a Ringer pulse) was subtracted to display the net effect. The blue line represents data regression performed with a 5th order polynomium.

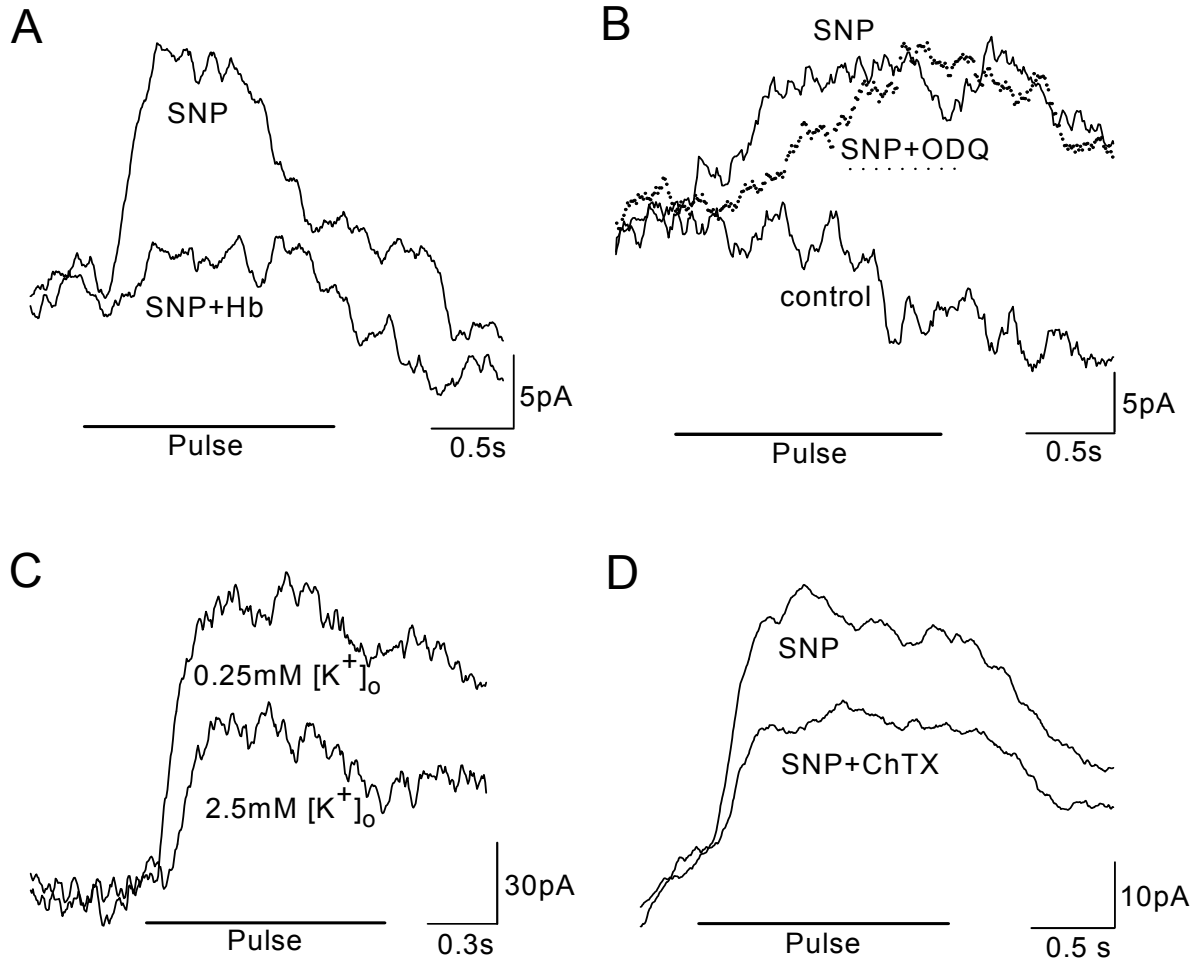

Fig. 12. NO induces a potassium current independent from cGMP.
A) The NO-scavenger hemoglobin (Hb; 10 mg/ml) diminished the outward current triggered by SNP in *Caudiverbera* olfactory receptor neurons (n = 7). **B**) The guanylyl cyclase-inhibitor ODQ did not affect the SNP response (n = 4). The control displays only the voltage-gated current without stimulus pulse. **C**) The NO-induced current as measured in normal and low-potassium Ringer at –30 mV (n = 4). The voltage-gated currents were subtracted. **D**) The potassium channel blocker charybdotoxin (ChTX; 200 nM) reduced the effect of SNP on olfactory receptor neurons (n = 7). The displayed traces stem from experiments like the one in Fig. 11C, but only the currents during the depolarizing voltage step are shown.

Given the ionic distribution between the intra- and extracellular solution and the known voltage-dependent membrane conductances in olfactory receptor neurons [Schild, 1989; Delgado & Labarca, 1993], an outward current developing at negative membrane potentials is likely to be a potassium current. To test the hypothesis, the potassium concentration of the extracellular solution was transiently lowered to 0.25 mM, increasing the potassium gradient tenfold. Stimulation under this condition produced larger outward currents than in normal Ringer, confirming that the NO-induced current is principally carried by potassium (Fig. 12C). Along this line of evidence, the current was sensitive to the specific potassium channel blocker charybdotoxin (Fig. 12D), suggesting the activation of potassium channels by NO.

The dose-response relationship of this effect was obtained by subsequent trials with increasing pressure on the stimulus pipette. As displayed by Fig. 13, the curve is nearly linear between 0 and 0.6 bar, approaching a maximum at higher pressures.

3.6. NO activates a calcium-dependent potassium conductance

To characterize the conductances underlying the NO-effect, several ion channel blockers were applied together with the NO-donor SNP. 2 mM tetraethylammonium (TEA) reversibly abolished the NO-induced current and reduced the voltage-dependent currents (Fig. 14A). TEA blocks large-conductance calcium-dependent potassium (K_{Ca}) channels in submillimolar concentrations [$K_d \approx 0.14$-0.29 mM; see Latorre, 1994], but not small-conductance K_{Ca}-channels, which are insensitive to TEA. Iberiotoxin (IbTX), a specific blocker of large-conductance K_{Ca}-channels significantly reduced the NO-induced current at 100 nM (Fig. 14B). The fact that IbTX did not cause a total block at this concentration in spite of a reported K_d of ~ 1 nM in muscle cells [Candia et al., 1992] might be indicative of a lower IbTX sensitivity of the K_{Ca}-channels in this tissue, or of the participation of other potassium channels, possibly of intermediate conductance.

2 µM apamin, a potent specific blocker of small-conductance K_{Ca}-channels (K_d in the nanomolar range), did not reduce the NO-induced current significantly (Fig. 14C), arguing against a contribution of these channels to the observed effect.

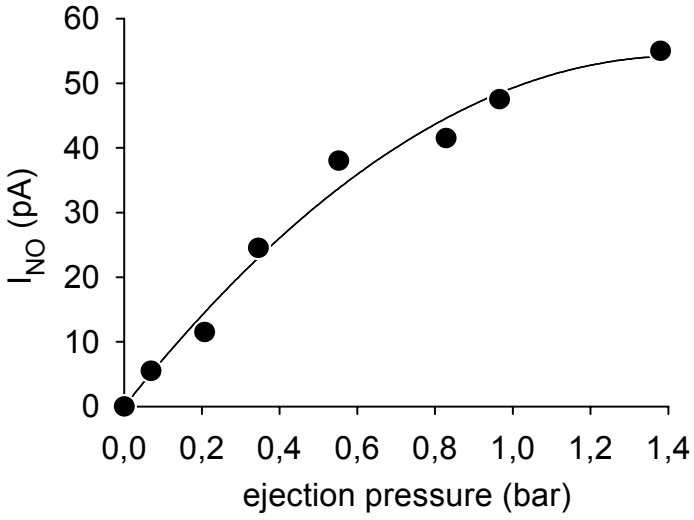

Fig. 13. Dose-dependence of the NO-effect. Net NO-induced currents of subsequent trials (intervals: 30 s) in a *Caudiverbera* olfactory receptor neuron are plotted against the ejection pressure of the picospritzer. Cells were stimulated by 1.5 s SNP-pulses during 3 s voltage steps to –30 mV. The solid line represents a second-order regression.

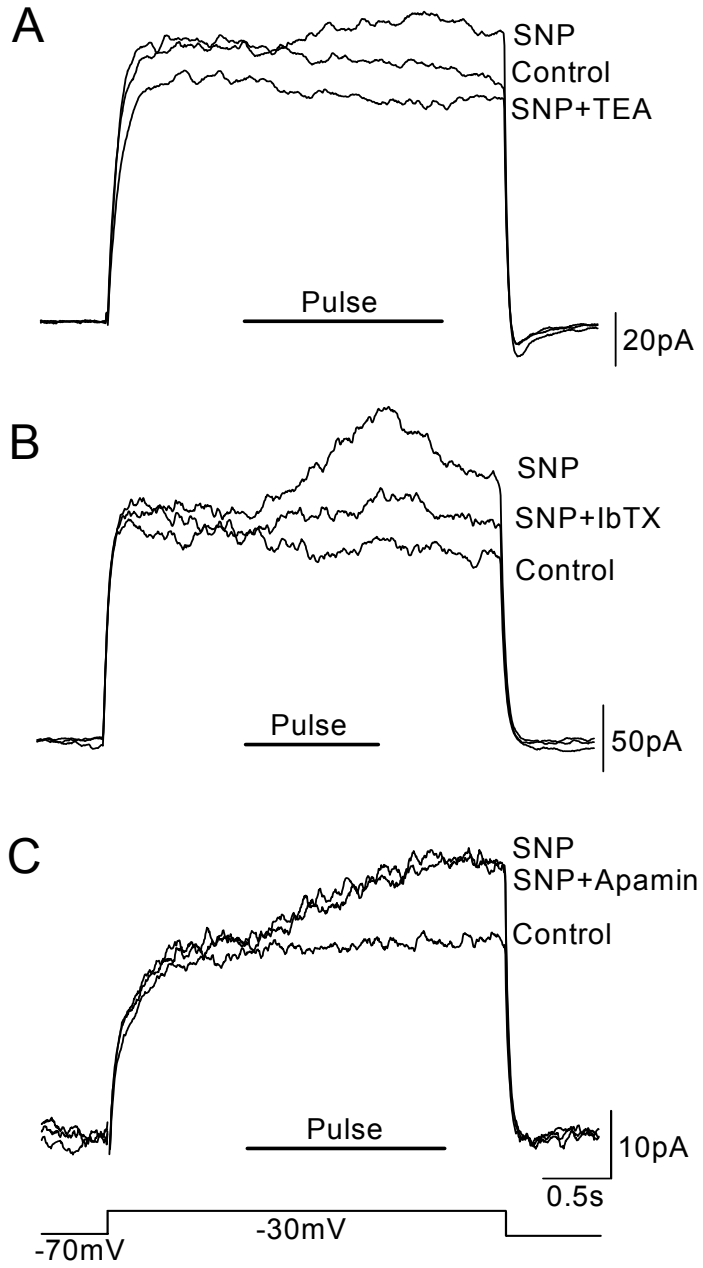

Fig. 14. The NO-effect is blocked by the potassium channel blockers TEA and IbTX, but not by apamin. **A**) Perfusion with 2 mM TEA. TEA abolished the NO-induced current and reduced the voltage-activated currents, as shown by the downward displacement of the lower trace (n = 7). **B**) Co-ejection of 100 nM IbTX with SNP (n = 8). **C**) Co-ejection of 2 µM apamin with SNP (n = 9). Recordings were obtained from voltage-clamped *Caudiverbera* olfactory receptor neurons during 3 s voltage-steps to –30 mV. Control traces were obtained by depolarizing steps in the absence of a stimulus.

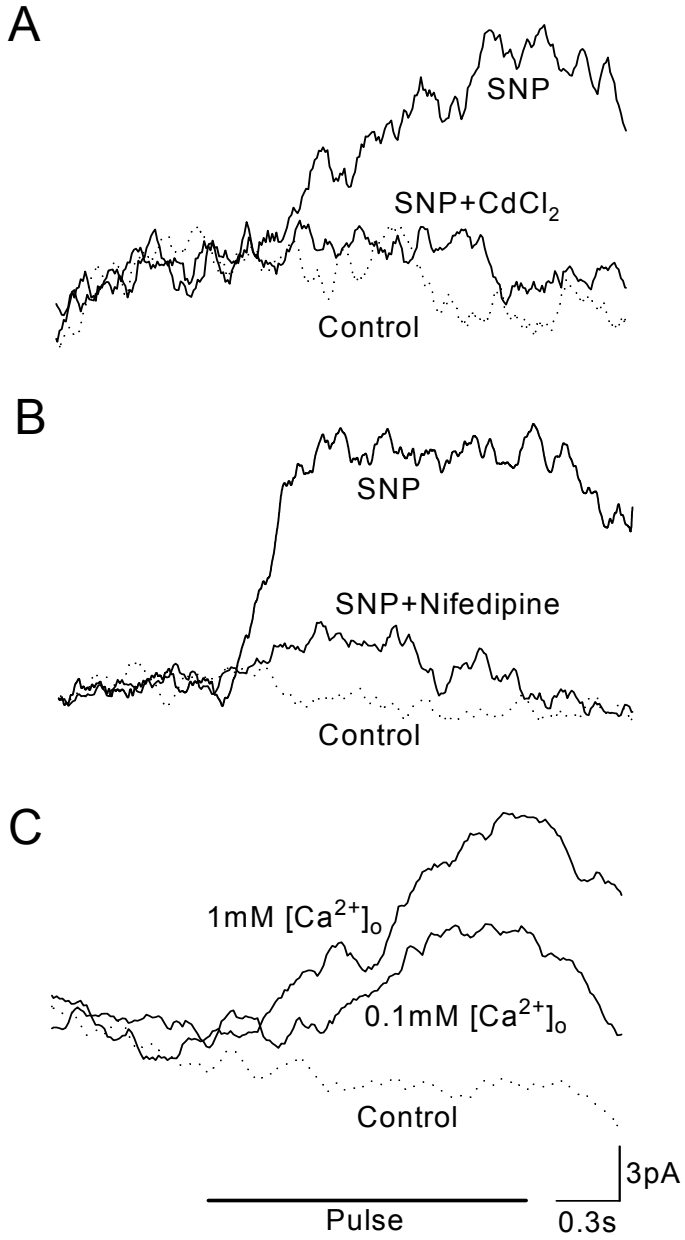

Fig. 15. The NO-induced current is dependent on calcium influx. **A**) Perfusion with the calcium channel blocker cadmium chloride ($CdCl_2$; 100 µM; n = 4). **B**) Perfusion with 50 µM nifedipine, a blocker of L-type calcium channels (n = 5). **C**) Exchange of 1 mM external calcium by 0.1 mM reduced the effect of an SNP-pulse applied in the same respective Ringer (n = 6). In all cases, the NO-induced current recovered. Controls (dotted lines) are in normal Ringer, without stimulus.

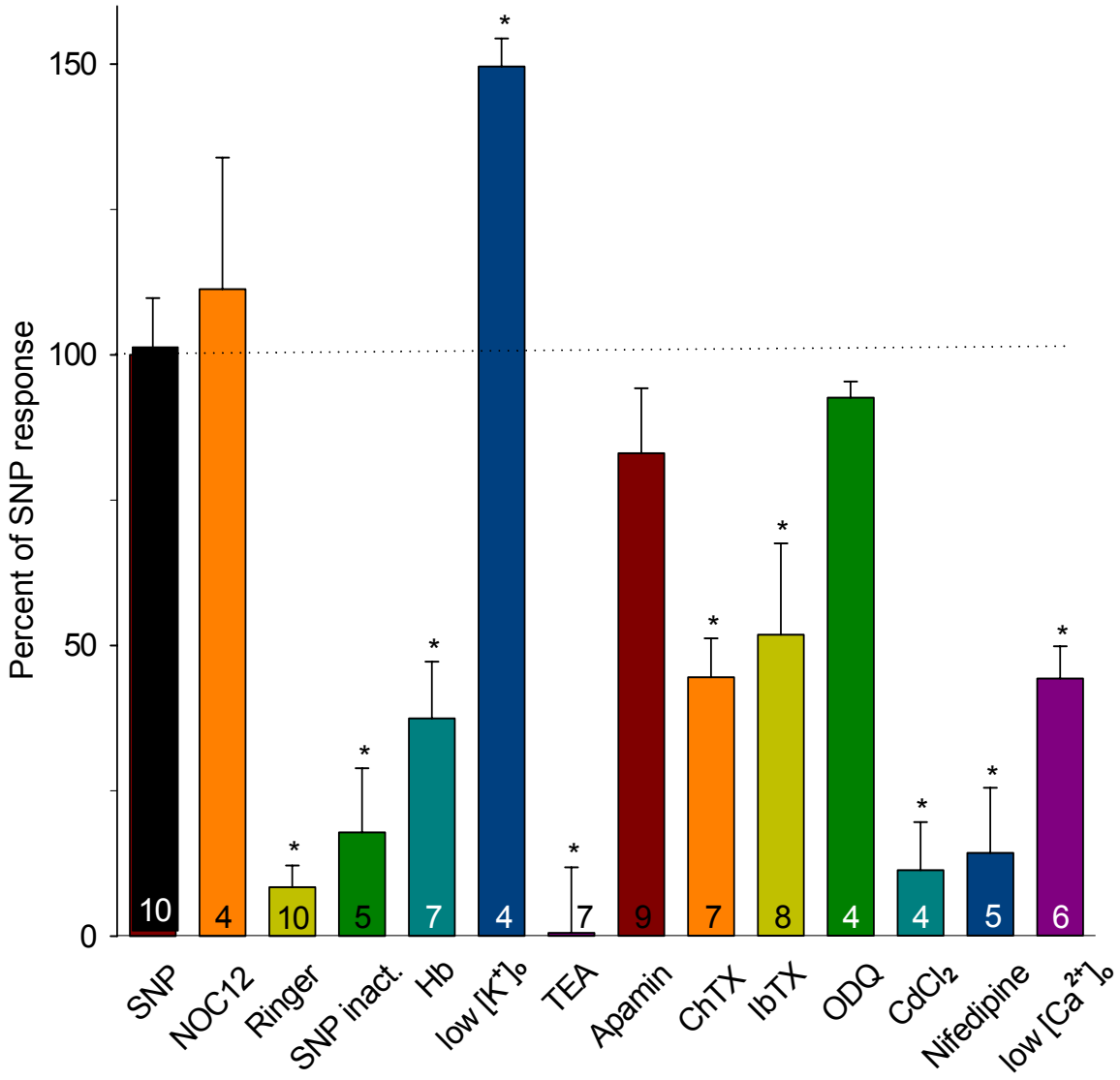

Fig. 16. Overview of the NO-responses of *Caudiverbera* olfactory receptor neurons under various experimental conditions. Bars (+ SEM) display the relative NO-induced net current amplitude at –30 mV under each tested condition, compared to SNP alone (black bar = 100%). Only experiments with at least partial recovery were considered, with numbers representing the total of cells analyzed. Asterisks indicate significant differences to the SNP-control according to the unpaired Student´s t-test ($p < 0.05$).

The graph summarizes that NO is the active component of the stimulus solution causing an outward current which is sensitive to certain potassium channel blockers and the external potassium concentration. ODQ did not diminish the NO-induced current, which was however affected by calcium channel blockers and external calcium.

3.7. The NO-induced potassium current is dependent on calcium influx

Possible mechanisms by which NO might open K_{Ca}-channels include a direct, covalent activation of these channels and an increase of intracellular calcium. To test the latter possibility, the neurons were stimulated with NO during perfusion with the calcium channel blockers cadmium and nifedipine. As demonstrated by representative traces in Figs. 15A and B, both cadmium and nifedipine largely eliminated the NO-induced potassium current, which nonetheless recovered completely after the end of perfusion. Experiments with low-calcium perfusion provided further evidence for an influx of that ion, as a tenfold reduction of external calcium significantly reduced the outward current (Fig. 15C). An overview of the pharmacological and ionic conditions used to investigate the NO-effect is shown as bar graph (Fig. 16).

The previous results predict that an inward current should be associated with the activation of the NO-induced potassium current, but in the experiments presented here, stimulation with SNP under normal ionic conditions did not cause visible inward currents, irrespective of the holding potential (Fig. 17A). Yet, NO has been reported to induce inward currents in *Xenopus* [Lischka & Schild, 1993] and the turtle [Inamura et al., 1998]. In those experiments, olfactory receptor neurons were subjected to prolonged bath perfusion with 10 mM SNP. To examine if continuous application of NO modified the cellular responses, olfactory receptor neurons from *Caudiverbera* were perfused with the NO-donor SNP during one minute (Fig. 17B). No inward currents could be discerned at –70 mV, a potential at which an activation of the cyclic nucleotide-gated channels is expected to produce a large current (equilibrium potential ~ 0 mV), but where potassium currents are very small due to their voltage-dependence and their equilibrium potential of ~ –100 mV. At –40 mV, the NO-induced outward current is clearly visible.

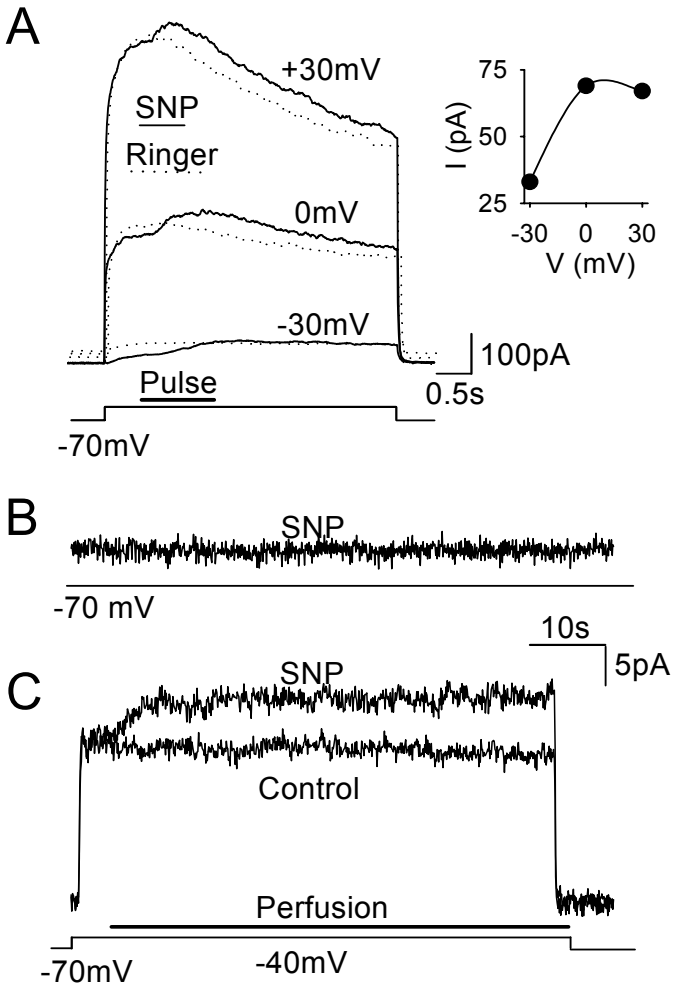

Fig. 17. NO-induced inward currents are generally not observed under standard experimental conditions. **A**) At –30, 0 and +30 mV, SNP induced outward currents. The absence of a tail current upon returning to the holding potential of –70 mV indicates that the cyclic nucleotide-gated conductance was not activated (reversal potential ≈ 0 mV), because the respective current would be large at that potential, whereas the voltage-gated channels are closed, and potassium is near its equilibrium potential (n = 55). **B**) An olfactory receptor neuron was held at –70 mV and microperfused with SNP during 1 min. No current was induced (n = 8). **C**) The same cell was stimulated at –40 mV, resulting in the activation of a sustained outward current.

Since the putative calcium current was not observable under normal conditions, the potassium of the internal solution was replaced with cesium, and 10 mM TEA was added to the bath, thus blocking all potassium conductances. Under these conditions, NO caused a small inward current at –30 mV in 9 out of 11 cells (average ≈ 0.5 pA; Fig. 18A). This inward current could also be seen after replacement of external sodium by N-methyl-d-glucamine (n = 2, not shown), indicating that calcium, and not sodium, was indeed the entering ion.

To visualize the rise in intracellular calcium that should occur as a consequence of the NO-induced inward current, calcium-imaging of *Caudiverbera* olfactory receptor neurons loaded with Fluo-3,AM was performed during stimulation with NO (Fig. 18B). In 6 out of 24 neurons, NO caused a transient fluorescence increase, indicative of an increment in intracellular calcium. The fact that a rise in intracellular calcium could only be observed in 25% of the cells, as opposed to 78% displaying the NO-induced potassium current, might be explained by the small magnitude of the calcium current. Altogether, these results support the interpretation that NO activates K_{Ca}-channels by triggering a calcium influx.

3.8. The NO-induced potassium current localizes to the soma

The fluorescence increase caused by NO under calcium imaging seemed evenly distributed throughout the cell body and was also present in cells without cilia (fluorescence in the cilia was not resolved), in agreement with the electrophysiological observation of the NO-induced potassium current in deciliated cells (Fig. 19A, B). These cells have lost their cilia during the dissociation process and do not transduce odors, but behave otherwise normally.

The localization of the activated conductance was further investigated by means of focal stimulation of intact isolated neurons (Fig. 19C). Puffs of SNP directed to the soma, where the voltage-gated channels reside [see Schild & Restrepo, 1998] generally yielded slightly larger currents than stimulation of the dendritic knob and the cilia, but the effect was present in all cases. Olfactory receptor neurons are thought to express a ciliary K_{Ca}-conductance which

participates in inhibitory odor responses [Morales et al., 1995], thus it cannot be excluded that this putative conductance is activated by NO as well and contributes to the overall NO-induced current. Alternatively, puffs directed at the cilia might reach the rest of the cell by diffusion, opening potassium channels in the dendrite and soma.

The cyclic nucleotide-gated (CNG) transduction channels are concentrated in the cilia, but can also be found in the soma at much lower densities [Kurahashi & Kaneko, 1991]. These channels are permeable to calcium and have been reported to be directly activated by NO [Broillet & Firestein, 1996a], suggesting their participation in the effect described here. Although the NO-induced potassium current is independent from the presence of cilia, it cannot be ruled out that it involves the somatic part of the CNG conductance. To test this hypothesis, LY83583, a blocker of CNG channels [Leinders-Zufall & Zufall, 1995], was added to the bath. Yet, the blocker did not impair prominent NO-effects (Fig. 19D), arguing against a significant involvement of the CNG conductance in the NO-induced response.

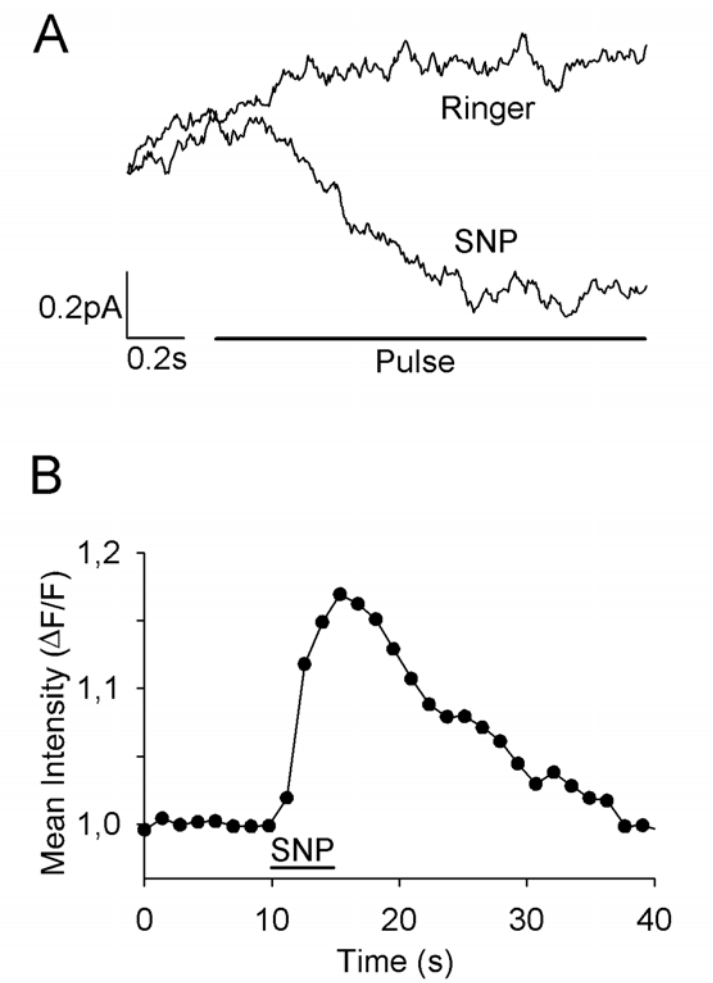

Fig. 18. NO causes calcium influx. **A**) Pulses of 10 mM SNP induced inward currents in *Caudiverbera* olfactory receptor neurons voltage-clamped at –30 mV after replacement of internal potassium by cesium and addition of 10 mM TEA to the external solution. Traces represent the average of eight experiments in one cell. Control puffs with Ringer had no effect. **B**) NO causes a rise in intracellular calcium. A 5 s pulse of SNP induced a fluorescence increase in a Fluo3,AM-loaded olfactory receptor neuron under confocal calcium-imaging (n = 6 out of 24). Mean pixel intensities integrated from the entire cell were recorded in 1 s-intervals and normalized with a bleaching curve constructed from two non-responsive cells.

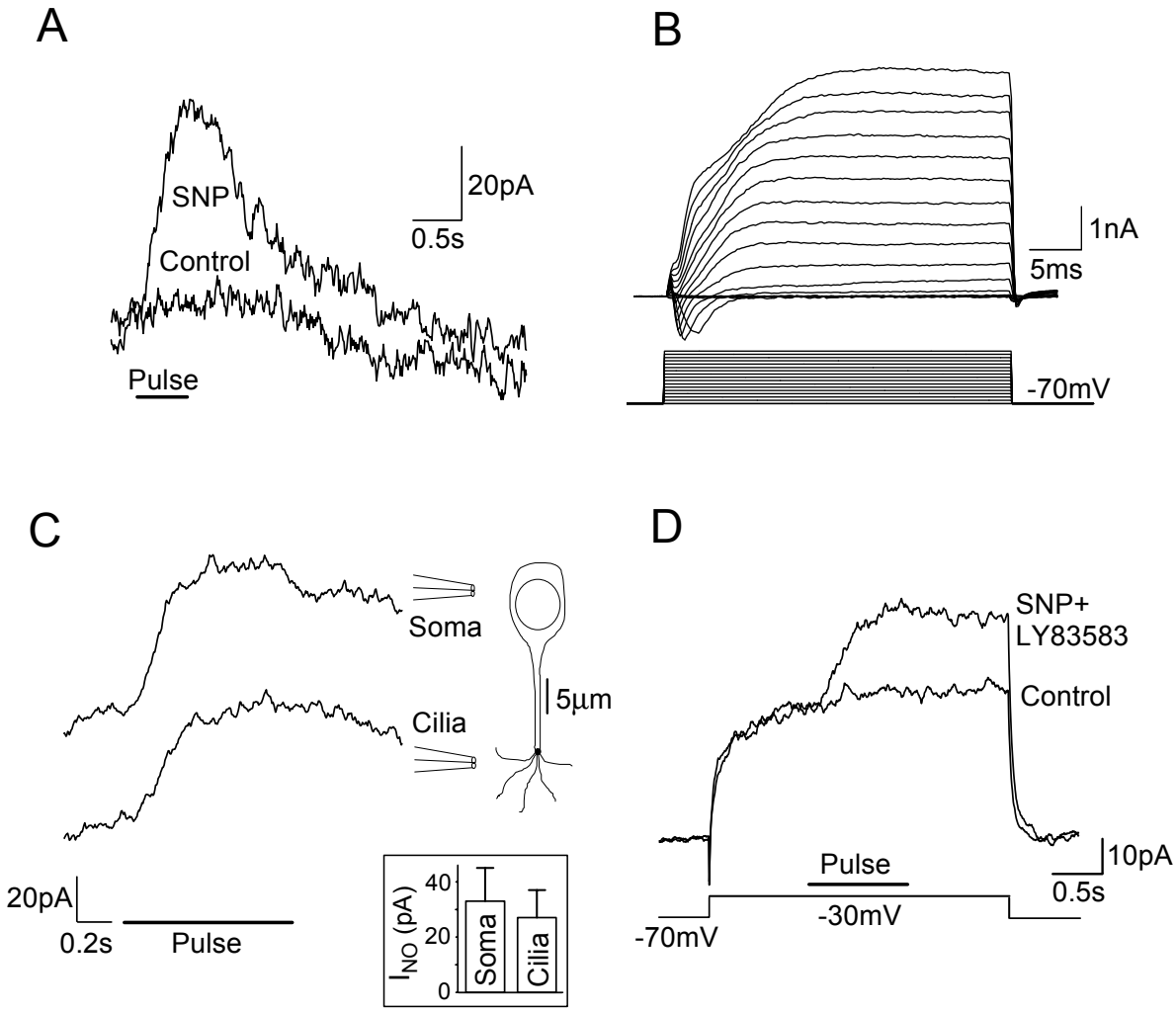

Fig. 19. The NO-induced potassium current is triggered in the soma. **A**) NO caused outward currents in olfactory receptor neurons without cilia. Control is with inactivated SNP (n = 18). **B**) The voltage-dependent currents of this neuron, induced by a series of voltage steps from –80 to +90 mV, display the normal behavior of a mature olfactory receptor neuron [Delgado & Labarca, 1993]. **C**) The NO-induced current is independent from the cyclic nucleotide-gated conductance. A fine ejection pipette (tip diameter ca. 1 µm) was used to apply SNP-pulses to the cilia and to the soma. If the effect involved the cyclic nucleotide-gated channels, it should be larger upon ciliary stimulation, which was not the case. Inset: Average peak current amplitudes induced by SNP-ejection onto the soma and the cilia at –30 mV (n = 4). **D**) The cyclic nucleotide-gated channel blocker LY83583 (20 µM in the bath) did not block the NO-induced current. In other experiments, co-ejection of LY83583 with SNP was equally ineffective (n = 5).

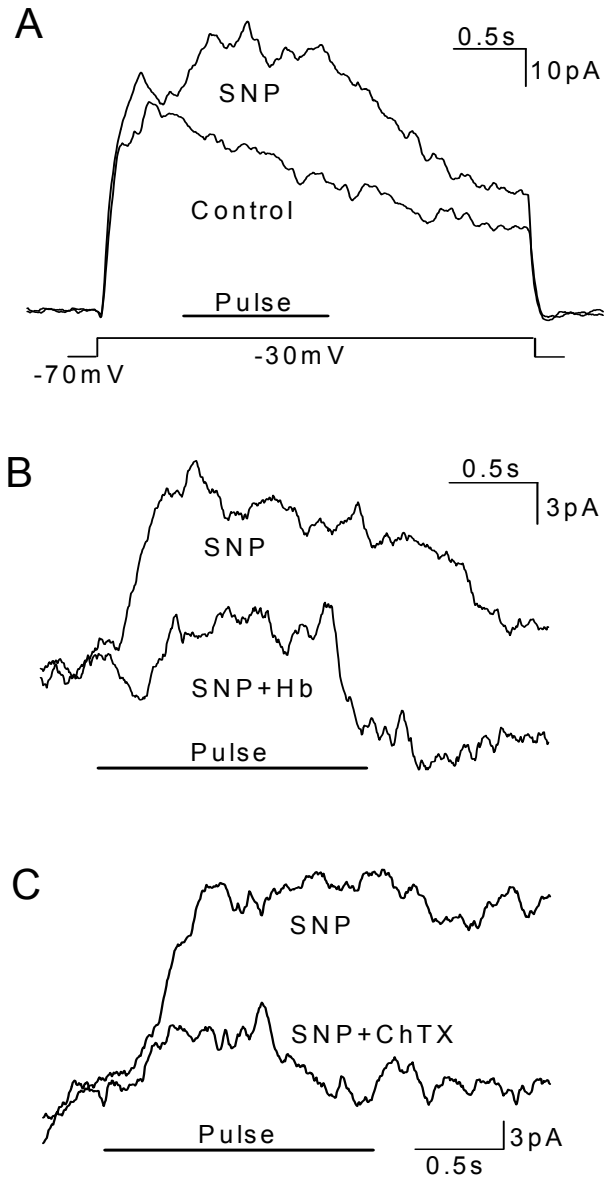

Fig. 20. *Xenopus* olfactory receptor neurons display a NO-induced potassium current comparable to *Caudiverbera*. **A**) A pulse of SNP caused a transient outward current compared to Ringer as control in a voltage-clamped *Xenopus* neuron. **B**) The NO-induced current was diminished by hemoglobin (10 mg/ml) in the stimulus solution. **C**) The NO-induced current was sensitive to the potassium channel blocker charybdotoxin.

3.9. In Xenopus and the rat, NO causes an effect comparable to Caudiverbera

To investigate whether the NO-induced current described here is also present in olfactory receptor neurons from other species, some essential experiments were repeated in *Xenopus* and the rat. As shown in Fig. 20, a pulse of the NO-donor SNP elicited an outward current in isolated olfactory receptor neurons from *Xenopus*. This current, which was observed in 18 out of 27 (67%) cells, was sensitive to the NO-scavenger hemoglobin and to the potassium channel blocker charybdotoxin, indicating that NO induced a potassium current as in *Caudiverbera*.

In the rat, pulses of the NO-donor SNP induced outward currents in 42% of the analyzed neurons (30 out of 72 cells (42%) from 20 animals; Fig. 21). Although less frequent, the effect seemed similar to the one described for *Caudiverbera*. Currents elicited by NO were positive over the whole voltage range tested and their averaged current-voltage relationship reminds of K_{Ca}-conductances (Fig. 21A inset). The current could be blocked by IbTX (Fig. 21B), but not by LY83583 (Fig. 21C). The presence of the soluble guanylyl cyclase inhibitor ODQ in the internal solution had no effect upon the NO-induced current (n = 3, not shown), indicating that cGMP was not involved. Under conditions where outward currents had been largely eliminated, a small inward current could be detected (≈ 0.5 pA), that was abolished by the calcium channel blocker cadmium (Fig. 21D).

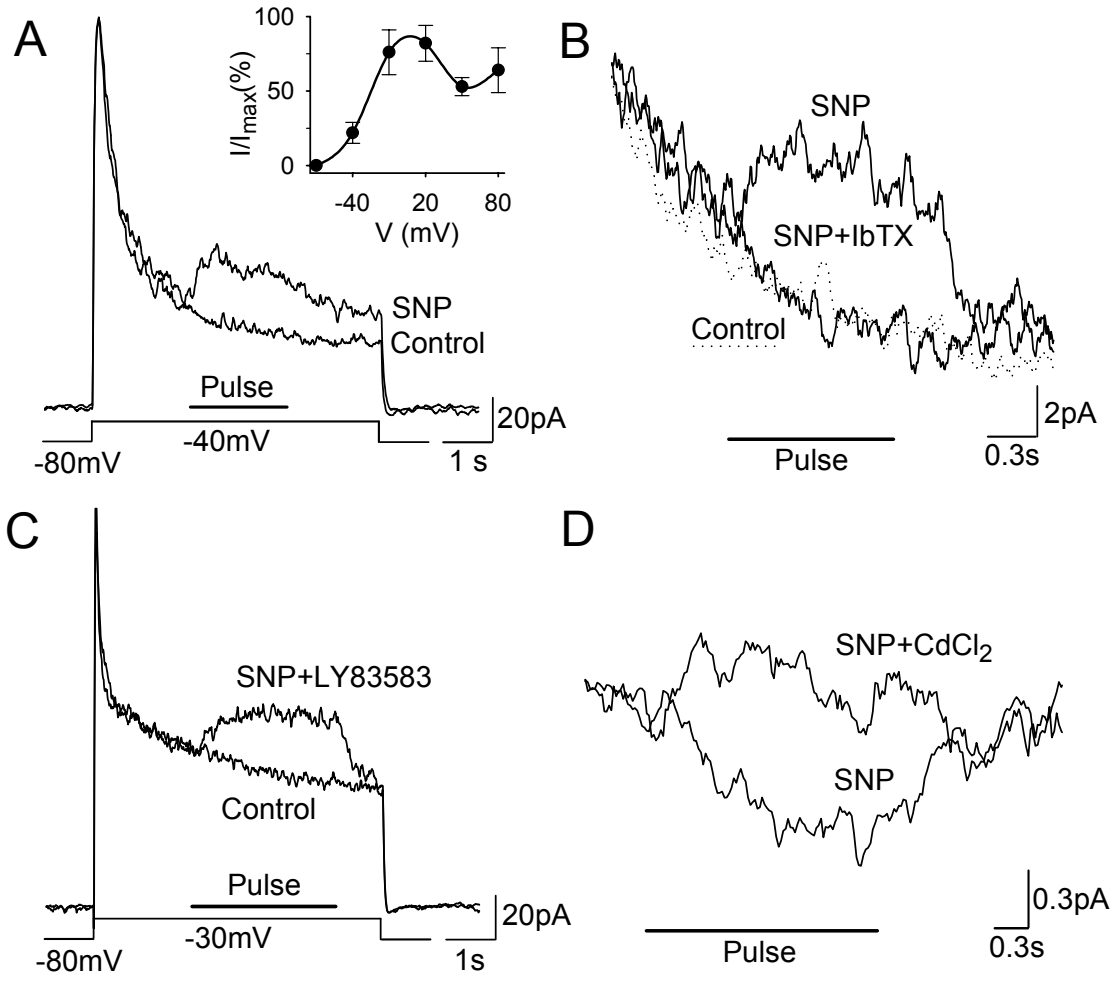

Fig. 21. NO elicits a similar effect in the rat. **A**) A 2 s pulse of 10 mM SNP, applied during a depolarizing voltage step to –40 mV, triggered a transient outward current. Control is without pulse. Inset: Current-voltage relation of the NO-induced current, averaged from five cells. Values (medium ± SEM) were obtained by a series of depolarizing steps of 30 ms duration during a SNP-pulse. The voltage-gated currents were subtracted and the net currents were normalized to the peak values. **B**) Co-ejection of the K_{Ca}-channel blocker IbTX (100 nM) with SNP. Recordings were obtained during 3 s voltage steps to –30 mV. Control (dotted line) is without pulse (n = 7). **C**) Co-ejection of 10 μM LY83583 with SNP (n = 4). **D**) With cesium instead of potassium in the internal solution and 10 mM TEA in the bath, SNP induced a small inward current at –30 mV, that could be blocked by co-ejection of 0.4 mM cadmium chloride. Traces are averaged from 3 experiments in one cell.

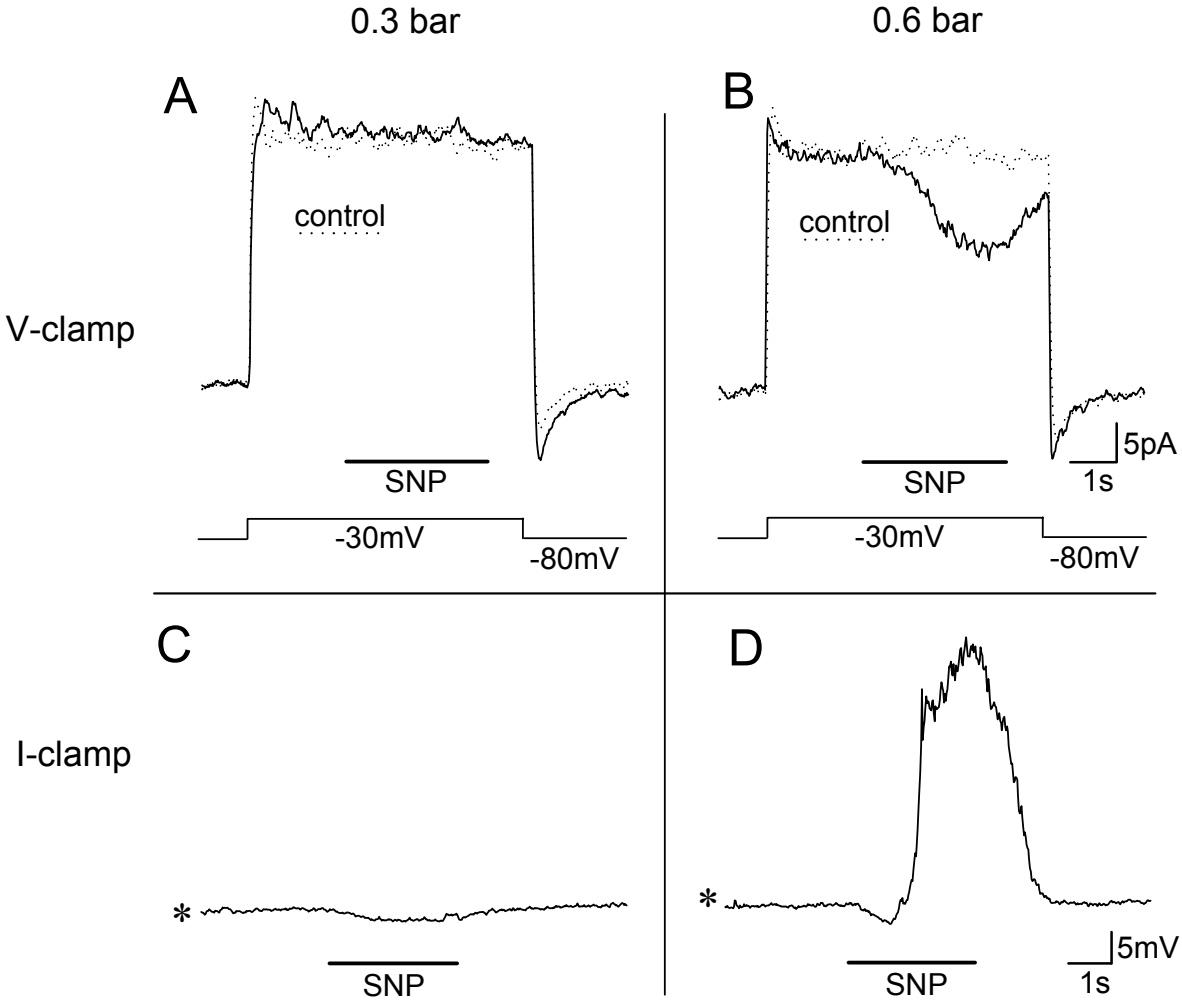

Fig. 22. NO-induced depolarizing inward currents were rarely observed in the rat. At low stimulus pressure, SNP caused no visible effect under voltage-clamp (**A**) and a small hyperpolarization under current-clamp (**C**) in this cell. **B**) With higher pressure, an inward current developed upon SNP-stimulation under voltage-clamp and a considerable membrane depolarization is observed under current-clamp (**D**). This depolarization is preceded by a short hyperpolarization that might correspond to the NO-induced potassium current of Fig. 21, suggesting that both effects may occur at the same time. Controls are without pulse.

3.10. High concentrations of NO induce inward currents

While investigating the NO-induced potassium current in the rat, very few times inward currents were observed upon stimulation with NO (n = 3 out of 54 cells). In the example shown in Fig. 22, the inward current is induced only at higher stimulus pressures. Under voltage clamp, NO triggered the current with a considerable latency of ~ 1 s. Under current clamp, the stimulus produced a significant membrane depolarization in the same cell.

Whereas NO-induced inward currents were rather exceptional under normal conditions, they were regularly observed upon NO-stimulation if cyclic AMP (cAMP) was added to the intracellular solution at subthreshold concentrations (Fig. 23A). In that case, the voltage-clamped cells responded to a pulse of SNP with a large inward current that returned to normal only several seconds after the end of the pulse. In control experiments, inactivated SNP did not produce any current. These data suggest that NO and cAMP both activate the cyclic nucleotide-gated transduction channel in an accumulative manner.

To check whether higher concentrations of NO could regularly induce an inward current by itself, even in the absence of cAMP, SNP was added to the intracellular solution. In this experimental mode, the NO-donor rapidly fills the entire neuron including the cilia after the establishment of the whole-cell mode. As shown in Fig. 23B, a large inward current was induced soon after the breaking of the patch seal. In subsequent experiments, GTP was replaced by ODQ in the internal solution, in order to eliminate the possibility of cGMP-synthesis by soluble guanylyl cyclase. The fact that NO caused an inward current independent from GTP and ODQ demonstrates that this NO-effect is not mediated by cGMP. Comparable currents were observed in complementary experiments with normal intracellular solution (not shown).

The NO-induced inward current frequently decreased after an initial peak, even with ongoing stimulation (Fig. 23A, C & D). This phasic-tonic shape of the current is probably due

to the inhibition of the cyclic nucleotide-gated conductance by intracellular calcium, which implies a negative feedback effect [Chen & Yau, 1994].

In odor detection, calcium enters the olfactory receptor neuron through the ciliary cyclic nucleotide-gated transduction conductance, activating in turn ciliary calcium-dependent chloride channels [Lowe & Gold, 1993]. To investigate whether the same occurred under NO-stimulation, and to discard the possibility that NO only activated the calcium-dependent chloride channels, the chloride channel blocker niflumic acid was added to the extracellular bath solution. Fig. 23D displays that NO still triggered an inward current, however with much more rapid recovering kinetics, suggesting that a slower chloride component of the current observed in Fig. 23C was eliminated by niflumic acid. This supports the hypothesis that NO opened the cyclic nucleotide-gated conductance and the entering calcium then activated the calcium-dependent chloride channels.

The characteristics of the NO-induced inward current were further analyzed by voltage ramps, that were applied during the peak of the current triggered by an SNP pulse (Fig. 24A). The resulting net current displays a current-voltage relationship (Fig. 24B) that is indistinguishable from that of the excitatory odor transduction current [Kurahashi, 1989], indicating that NO activated the same transduction conductances in these experiments.

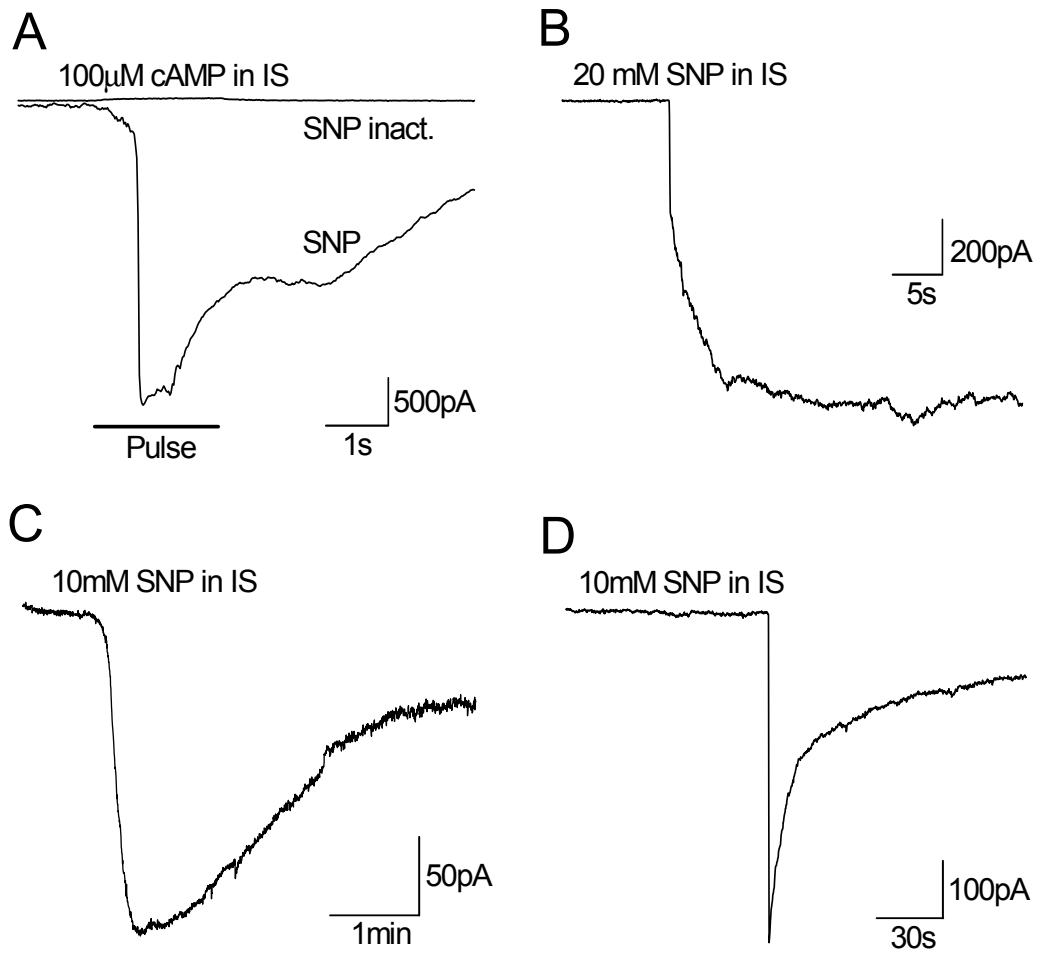

Fig. 23. High NO induced inward currents in rat olfactory receptor neurons.
A) 100 µM cyclic AMP in the intracellular solution (IS) did not induce significant currents on its own in voltage clamped rat olfactory receptor neurons at –80 mV. Stimulated with an SNP-pulse, a very large transient inward current develops, suggesting that only the united action of cAMP and NO led to the opening of the cyclic nucleotide-gated conductance (n = 5). **B**) 20 mM SNP in the intracellular solution triggered a large inward current without further stimulus. **C**) With 10 mM SNP and the guanylyl cyclase inhibitor ODQ (2 µM) in the internal solution, a large inward current is observed, indicating that NO did not act through cGMP (n = 3). **D**) In identical conditions as in (C), but with the chloride channel blocker niflumic acid in the extracellular solution (50 µM), this inactivation occurs more rapidly, suggesting that a slower chloride component has been blocked by niflumic acid.

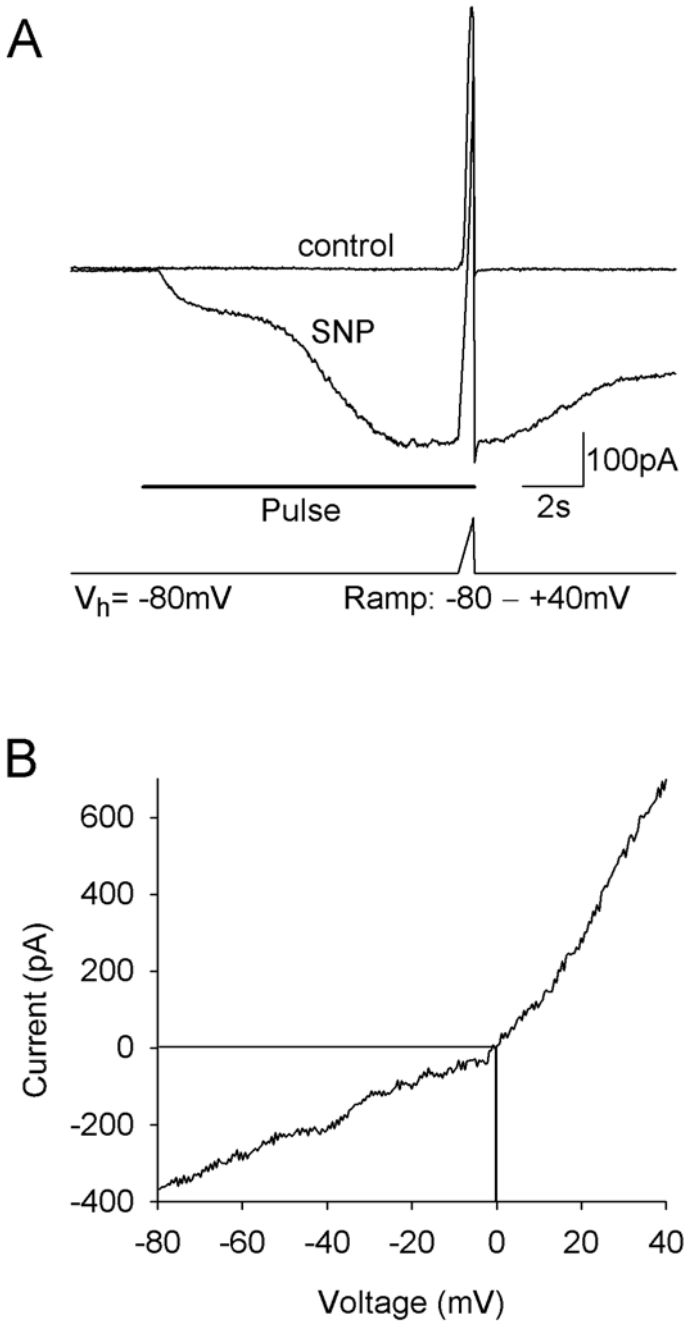

Fig. 24. The current-voltage relation of the NO-induced inward current.
A) To obtain the current-voltage relation of the NO-induced inward current, voltage ramps were applied during the peak of the current triggered by an SNP-pulse in a cell patch-clamped with 100 µM cyclic AMP in the intracellular solution. In a previous control experiment, the SNP-pulse was omitted. The control-ramp current was subtracted from the trial-ramp current and the suppression of the voltage-gated currents by SNP has been subtracted according to the methods described in Sanhueza & Bacigalupo [1999], to obtain the net current-voltage relation of the NO-induced current (**B**). This relation is linear at positive potentials, slightly outward rectifying and passes through zero, as does the excitatory odor transduction current.

4. Discussion

The histochemical data presented here show that NADPHd, a marker for NOS, is expressed in the olfactory epithelium in a steeply rising number of receptor neurons during the first month after birth. Although the exact densities of neurons in the olfactory epithelium are not known, previous reports indicate an increase from ~900 to ~1300 neurons per mm of section length from P1 to P21 [Weiler & Farbman, 1997], or a rise by ~80% between P0 and P10 [Sakashita et al., 1995]. Therefore, the time dependence of the NADPHd staining pattern with its more than tenfold increase of labeled neurons does not merely reflect the overall development of the olfactory epithelium. This developmental pattern implies that the massive onset of NADPHd expression coincides with the onset of olfaction.

NADPHd was used as a marker for NOS [Dawson et al., 1991; Hope et al., 1991]. The specificity of this histochemical method, although probably better than that of commercial NOS antibodies [Coers et al., 1998], has been questioned, among other reasons due to its cross-reaction with the enzyme P450, which shares strong sequence homology with NOS. P450 is indeed expressed in the olfactory epithelium, but histological investigations with specific antibodies recognized the enzyme predominantly in sustentacular cells and Bowman glands, although low levels of immunoreactivity were also found in the receptor neuron layer [Kishimoto et al., 1993; Chen et al., 1992].

The finding that the strong NADPHd reaction of the sustentacular cells and Bowman glands vanished with prolonged fixation, while the neuronal staining remained, suggests that only the fixation-sensitive NADPHd reaction represents P450. In line with that argument, comparisons of NADPHd and P450 immunoreactivity in rat brain yielded, with few exceptions, no co-localization [Norris et al., 1994], suggesting that neuronal NADPHd staining is generally not due to P450. Finally, the sensitivity of our stainings to DPIP indicated that they are of a different nature than the NADPHd reaction observed in the

glomeruli of the olfactory bulb, which is insensitive to DPIP and probably not due to NOS [Kishimoto et al., 1993; Spessert et al., 1994]. Altogether, these data support the notion that the NADPHd reactivity of the rat olfactory receptor neurons corresponds to NOS, although they do not represent final proof and cannot completely exclude the possibility that NADPHd represents P450 or a different, hitherto unidentified protein. If NADPHd were P450, it could possibly serve such purposes as the elimination of xenobiotics or CO synthesis for neuronal signaling [Leinders-Zufall et al., 1995], although a role of CO as neural messenger has never been firmly established [reviewed by Barañano et al., 2001].

Using immunohistochemistry, NOS has been found to be transiently expressed in rodent olfactory epithelium during embryonic development [Roskams et al., 1994; Arnhold et al., 1997]. However, NOS expression ceased shortly after birth. This contradiction with the staining patterns of the NOS marker NADPHd presented here might possibly be explained by a switch in the splicing variant or NOS isoform at some developmental stage, which would require a different antibody for its recognition. NOS has also been found in apical dendrites of bovine olfactory receptor neurons [Wenisch et al., 2000], and strong NADPHd expression co-localized with the NOS immunoreactivity in these cellular compartments.

These histological data concerning NOS in the olfactory epithelium support an involvement of NO within the physiology of olfactory receptor neurons. Therefore it was essential to investigate whether NO directly exerts a physiological effect upon these cells. The evidence presented here shows that NO may activate diverse olfactory receptor neuron membrane conductances, leading either to hyperpolarization or depolarization of the membrane potential.

The somatic potassium conductance underlying the observed membrane hyperpolarization is opened by NO in a cGMP-independent mechanism that involves calcium influx. The calcium-dependence of this effect, its current-voltage relationship and partial block by nanomolar charybdotoxin indicate the activation of a K_{Ca}-conductance by NO.

This conductance is also sensitive to iberiotoxin and TEA, but not to apamin (Fig. 14), suggesting K_{Ca}-channels of large or intermediate, but not small conductance [Candia et al., 1992; Cai et al., 1998]. Whole cell voltage-clamp studies have shown the presence of a K_{Ca}-conductance in the soma of olfactory receptor neurons from *Xenopus* and *Caudiverbera* [Schild, 1989; Delgado & Labarca, 1993]. Furthermore, a somatic K_{Ca}-channel with a unitary conductance of 130 pS and strong calcium-dependence has been described in mouse olfactory receptor neurons [Maue & Dionne, 1987].

Calcium involved in the activation of the NO-induced potassium current may enter the cell through calcium-permeant channels, or it may be released from internal stores. The observed effects of cadmium, nifedipine and a low external calcium concentration are consistent with the notion that NO causes calcium influx, which in turn activates K_{Ca}-channels. Direct measurements of NO-induced inward currents and calcium-imaging experiments supported that hypothesis. The question of how NO triggers calcium influx remains to be investigated, but the short latency between stimulus and onset of the NO-induced current ($\geq$ 30 ms) supports a direct covalent reaction rather than the involvement of an enzymatic pathway. Redox modulation of calcium currents by NO has already been reported for sympathetic neurons and heart muscle cells [Chen & Schofield, 1993; Campbell et al., 1996].

Calcium entry is also a key step in olfactory transduction. This raises the question of why a NO-induced calcium influx does not activate calcium-dependent chloride channels, as occurs during odor responses [Lowe & Gold, 1993]. One possibility is the existence of a spatial separation between the two calcium-entry pathways. Indeed, the experiments with focal stimulation indicated that the potassium current is larger after NO-stimulation of the soma, where calcium-dependent chloride channels would not be expected. Two calcium conductances have been described in olfactory receptor neurons: A somatic, voltage-dependent calcium conductance [Schild, 1989; Delgado & Labarca, 1993] and the cyclic

nucleotide-gated (CNG) conductance confined principally to the cilia. The results presented in this work support a calcium entry via the somatic channels (Fig. 19), because: 1) The effect is present in cells that have lost their cilia. 2) In cells with cilia somatic stimulation triggers larger currents than ciliary stimulation, although the density of the CNG channels is much lower in the soma. 3) High doses of the CNG channel blocker LY83583 did not block the NO-induced current.

On the other hand, Broillet & Firestein [1996[a], 1997] reported direct opening of native olfactory CNG channels from the tiger salamander and the rat as well as activation of recombinantly expressed rat α- and β-homomeric and α/β-heteromeric CNG channels by NO. The mechanism was shown to consist in the S-nitrosylation of a cysteine-residue in the carboxy-linker region involved in CNG channel gating [Broillet, 2000]. Intriguingly, a recent paper claimed exactly the opposite, namely inhibition of the CNG conductance by NO [Lynch, 1998]. In this work, macro-patches were excised from the olfactory knob of rat olfactory receptor neurons and stimulated with NO. Both studies present clean data with the necessary controls, and there is no obvious explanation for the different results.

As the whole-cell consequences of NO-actions on the CNG conductance were not demonstrated in any of these publications (Fig. 7 in Broillet & Firestein, 1996[a] is not convincing because of the unstable baseline, suggesting a leaky patch seal), experiments were designed to investigate the effect(s) of NO on the CNG conductance in the whole-cell patch clamp mode.

To that end, rat olfactory receptor neurons were voltage-clamped at –80 mV, a potential where the K_{Ca}-channels remain closed due to their voltage-dependence, but where the opening of the CNG transduction conductance produces large inward currents [Kurahashi, 1989]. cAMP was added to the intracellular solution to activate the transduction conductance, and NO was applied through pulses of NO-donors to investigate how it affected the resulting current.

If the used cAMP concentration was sufficient to induce an inward current, NO caused either no significant effect, or an additional activation (n = 5, not shown). However, if the cell did not respond to cAMP alone, which was frequently observed, an additional pulse of NO was able to trigger a large inward current (Figs 23A, 24A). These data, and the observation that high doses of NO in the intracellular solution caused inward currents even in the absence of cAMP, support the notion of a NO-activation of the CNG conductance, and they are in disagreement with the NO-inhibition reported by Lynch [1998].

Interestingly, the two previous whole cell patch-clamp studies reporting NO-induced inward currents in olfactory receptor neurons also concluded an involvement of cGMP [Lischka & Schild, 1993; Inamura et al., 1998], proposing NO-activation of soluble guanylyl cyclase and discarding a direct NO-effect. However, the above studies lack a pharmacological characterization of the observed currents, and the hypothesis of a NO/cGMP-system is principally based on the comparison of SNP- with cGMP-effects. Therefore, their data do not appear sufficient to reject a direct NO-activation of the CNG conductance as demonstrated in this work. On the other hand, a small contribution of a hypothetical NO/cGMP-system cannot be excluded either. The outward potassium current described here was not observed in these recordings since they were done at a holding potential (–70 mV) too close to the potassium equilibrium potential.

It is concluded that NO may open both the somatic K_{Ca}-conductance and the ciliary CNG channels in olfactory receptor neurons, and whether the membrane potential is hyper- or depolarized depends on the localization of the stimulus, on the intracellular calcium concentration and on the membrane potential itself. Accordingly, NO may produce both an increase and a decrease of the action potential frequency of the olfactory receptor neuron, depending on its momentary state of activity.

Assuming that the endogenous source of NO resides within the olfactory receptor neurons themselves, what might be the function of NO-signaling within the olfactory epithelium?

The existing data do not yet provide sufficient clues to answer this question. On the one hand, the absence of the NOS-marker NADPH diaphorase from the dendritic and ciliary compartments of olfactory receptor neurons from adult rats argues against the previously proposed hypothesis of an alternative transduction pathway mediated by NO [Breer & Shepherd, 1993]. On the other hand, the electrophysiological data presented here are suggestive of a participation of NO within transduction-related processes such as spike-frequency adaptation, but such a putative function remains to be demonstrated.

Recently, cGMP was reported to inhibit growth cone movements of olfactory receptor neurons through the opening of the CNG conductance and the resulting calcium influx [Kafitz et al., 2000]. Since NO has been implicated in filopodial steering [Van Wagenen & Reeder, 1999; 2001], induces neuronal growth cone collapse in rat dorsal root ganglion neurons [Hess et al., 1993] and stops growth during neuronal differentiation in PC12 cells [Peunova & Enikolopov, 1995], it might also exert a similar function in olfactory receptor neurons, involving the opening of growth cone CNG channels. Whether the putative NO-activation of these channels occurs through cGMP or in a direct manner remains to be established, but even a two-way action would not be without precedents, since vascular smooth muscle cells are relaxed by NO in both a cGMP-dependent process and through direct sulphhydril modification of K_{Ca}-channels [Bolotina et al., 1994].

In conclusion, the present data support an involvement of NO in the development of the olfactory epithelium and demonstrate direct effects of NO on olfactory receptor neuron membrane conductances. Future research will have to establish the precise functions of this gaseous messenger in olfaction.

5. References

1. Arnhold S, Andressen C, Bloch W, Mai JK and Addicks K. 1997. NO synthase-II is transiently expressed in embryonic mouse olfactory receptor neurons. *Neurosci Lett* **229**:165-168

2. Barañano DE, Ferris CD and Snyder SH. 2001. Atypical neural messengers. *Trends Neurosci* **24**:99-106

3. Bolotina VM, Najibi S, Palacino JJ, Pagano PJ and Cohen RA. 1994. Nitric oxide directly activates calcium-dependent potassium channels in vascular smooth muscle. *Nature* **368**:850-53

4. Bredt DS and Snyder SH. 1989. Nitric oxide mediates glutamate-linked enhancement of cGMP levels in the cerebellum. *Proc Natl Acad Sci USA* **86**:9030-9033

5. Bredt DS and Snyder SH. 1994. Transient Nitric Oxide Synthase Neurons in Embryonic Cerebral Cortical Plate, Sensory Ganglia, and Olfactory Epithelium. *Neuron* **13**:301-313

6. Breer H and Shepherd GM. 1993. Implications of the NO/cGMP system for olfaction. *Trends Neurosci* **16**:5-9

7. Breer H, Klemm HT and Boekhoff I. 1992. Nitric oxide mediated formation of cyclic GMP in the olfactory system. *Neuroreport* **3**:1030-1032

8. Broillet M-C and Firestein S. 1996[a]. Direct Activation of the Olfactory Cyclic Nucleotide-gated Channel through Modification of Sulfhydryl Groups by NO Compounds. *Neuron* **16**:377-385

9. Broillet M-C and Firestein S. 1996[b]. Gaseous Second Messengers in Vertebrate Olfaction. *J Neurobiol* **30**:49-57

10. Broillet M-C and Firestein S. 1997. β Subunits of the Olfactory Cyclic Nucleotide-Gated Channel form a Nitric Oxide Activated Ca^{2+} Channel. *Neuron* **18**:951-958

11. Broillet M-C. 2000. A single intracellular cysteine residue is responsible for the activation of the olfactory cyclic nucleotide-gated channel by NO. *J Biol Chem* **275**:15135-41

12. Cai S, Garneau L and Sauve R. 1998. Single-channel characterization of the pharmacological properties of the K(Ca2+) channel of intermediate conductance in bovine aortic endothelial cells. *J Membr Biol* **163**:147-158

13. Campbell DL, Stamler JS and Strauss HC. 1996. Redox modulation of L-type calcium channels in ferret ventricular myocytes. Dual mechanism regulation by nitric oxide and S-nitrosothiols. *J Gen Physiol* **108**:277-293

14. Candia S, Garcia ML and Latorre R. 1992. Mode of action of iberiotoxin, a potent blocker of the large conductance Ca^{2+}-activated K^{+} channel. *Biophys J* **63**:583-590

15. Chen TW and Yau KW. 1994. Direct modulation by Ca^{2+}-calmodulin of cyclic nucleotide-activated channel of rat olfactory receptor neurons. *Nature* **368**:545-548

16. Chen Y, Getchell ML, Ding X and Getchell TV. 1992. Immunolocalization of two cytochrome P450 isozymes in rat nasal chemosensory tissue. *Neuroreport* **3**:749-752

17. Chen C and Schofield GG. 1993. Nitric oxide modulates Ca^{2+} channel currents in rat sympathetic neurons. *Eur J Pharmacol* **243**:83-86

18. Coers W, Timens W, Kempinga C, Klok PA and Moshage H. 1998. Specificity of Antibodies to Nitric Oxide Synthase Isoforms in Human, Guinea Pig, Rat, and Mouse Tissues. *J Histochem Cytochem* **46**:1385-1391

19. Dawson TM, Bredt DS, Fotuhi M, Hwang PM and Snyder SH. 1991. Nitric oxide synthase and neuronal NADPH diaphorase are identical in brain and peripheral tissues. *Proc Natl Acad Sci USA* **88**:7791-7801

20. Delgado R and Labarca P. 1993. Properties of whole cell currents in isolated olfactory neurons from the Chilean toad *Caudiverbera caudiverbera*. *Am J Physiol* **264**:C1418-1427

21. Dellacorte C, Huque T, Wysocki L and Restrepo D. 1995. NADPH diaphorase staining suggests localization of nitric oxide synthase within mature vertebrate olfactory neurons. *Neurosci* **66**:215-225

22. Eliasson MJL, Blackshaw S, Schell MJ and Snyder SH. 1997. Neuronal nitric oxide synthase alternatively spliced forms: Prominent functional localizations in the brain. *Proc Natl Acad Sci USA* **94**:3396-3401

23. Garthwaite J and Boulton CL. 1995. Nitric Oxide Signaling in the Central Nervous System. *Annu Rev Physiol* **57**:683-706

24. Hamill OP, Marty E, Sakmann B and Sigworth FJ. 1981. Improved patch-clamp techniques for high resolution current recording from cells and cell-free membrane patches. *Pfluegers Arch* **391**:85-100

25. Hanazawa T, Konnu A, Kaneko T, Tanaka K, Ohshima H, Esumi H and Chiba T. 1994. Nitric oxide synthase-immunoreactive nerve fibers in the nasal mucosa of the rat. *Brain Res*. **657**:7-13

26. Hess DT, Patterson SI, Smith DS and Skene JH. 1993. Neuronal growth cone collapse and inhibition of protein fatty acylation by nitric oxide. *Nature* **366**:562-565

27. Hope BT, Michael GJ, Knigge KM and Vincent SR. 1991. Neuronal NADPH diaphorase is a nitric oxide synthase. *Proc Natl Acad Sci USA* **88**:2811-2814

28. Huard JMT, Youngentob SL, Goldstein BJ, Luskin MB and Schwob JE. 1998. Adult Olfactory Epithelium Contains Multipotent Progenitors That Give Rise to Neurons and Non-Neural Cells. *J Comp Neurol* **400**:469-486

29. Inamura K, Kashiwayanagi M and Kurihara K. 1998. Effects of cGMP and sodium nitroprusside on odor responses in turtle olfactory sensory neurons. *Am J Physiol* **275**:C1201-1206

30. Jaffrey SR, Erdjument-Bromage H, Ferris CD, Tempst P and Snyder SH. 2001. Protein S-nitrosylation: a physiological signal for neuronal nitric oxide. *Nat Cell Biol* **3**:193-197

31. Kafitz KW, Leinders-Zufall T, Zufall F and Greer CA. 2000. Cyclic GMP evoked calcium transients in olfactory receptor cell growth cones. *NeuroReport* **11**:677-681

32. Kishimoto J, Keverne EB, Hardwick J and Emson PC. 1993. Localization of Nitric Oxide Synthase in the Mouse Olfactory and Vomeronasal System: a Histochemical, Immunological and *In Situ* Hybridization Study. *Eur J Neurosci* **5**:1684-1694

33. Kulkarni AP, Getchell TV and Getchell ML. 1994. Neuronal Nitric Oxide Synthase Is Localized in Extrinsic Nerves Regulating Perireceptor Processes in the Chemosensory Nasal Mucosae of Rats and Humans. *J Comp Neurol* **345**:125-138

34. Kurahashi T and Kaneko A. 1991. High density cAMP-gated channels at the ciliary membrane in the olfactory receptor cell. *NeuroReport* **2**:5-8

35. Kurahashi T. 1989. Activation by odorants of a cation-selective conductance in the olfactory receptor cell isolated from the newt. *J Physiol* **419**:177-192

36. Latorre R. 1994. Molecular Workings of Large Conductance (Maxi) Ca^{2+}-Activated K^{+} Channels. In: Handbook of Membrane Channels. C. Paracchia, editor. pp. 79-102. Academic Press, Inc.

37. Lee SH, Iwanaga T, Hoshi O, Adachi I and Fujita T. 1995. Nitric Oxide Synthase in Rat Nasal Mucosa; Immunohistochemical and Histochemical Localization. *Acta Otolaryngol* **115**:823-829

38. Leinders-Zufall T and Zufall F. 1995. Block of Cyclic Nucleotide-Gated Channels in Salamander Olfactory Receptor Neurons by the Guanylyl Cyclase Inhibitor LY83585. *J Neurophys* **74**:2759-2762

39. Leinders-Zufall T, Shepherd GM and Zufall F. 1995. Regulation of Cyclic Nucleotide-Gated Channels and Membrane Excitability in Olfactory Receptor Cells by Carbon Monoxide. *J Neurophys* **74**:1498-1508

40. Lischka FW and Schild D. 1993. Effects of nitric oxide upon olfactory receptor neurones in *Xenopus laevis*. *NeuroReport* **4**:582-584

41. Lowe G and Gold GH. 1993. Nonlinear amplification by calcium-dependent chloride channels in olfactory receptor cells. *Nature* **366**:283-286

42. Lynch JW. 1998. Nitric Oxide Inhibition of the Rat Olfactory Cyclic Nucleotide-Gated Cation Channel. *J Membrane Biol* **165**:227-234

43. Malnic B, Hirono J, Sato T and Buck LB. 1999. Combinatorial receptor codes for odors. *Cell* **96**:713-23

44. Margolis FL. 1985. Olfactory marker protein: From PAGE band to cDNA clone. *Trends Neurosci* **8**:542-546

45. Marletta MA. 1994. Nitric oxide synthase: Aspects concerning structure and catalysis. *Cell* **78**:927-930

46. Matsumoto T, Nakane M, Pollock JS, Kuk JE and Forstermann U. 1993. A correlation between soluble brain nitric oxide synthase and NADPH-diaphorase is only seen after exposure of the tissue to fixative. *Neurosci Lett* **155**:61-64

47. Maue RA and Dionne V. 1987. Patch-Clamp Studies of Isolated Mouse Olfactory Receptor Neurons. *J Gen Physiol* **90**:95-125

48. Morales B, Labarca P and Bacigalupo J. 1995. A ciliary K^+ conductance sensitive to charybdotoxin underlies inhibitory responses in toad olfactory receptor neurons. *FEBS Lett* **359**:41-44

49. Norris PJ, Hardwick JP and Emson PC. 1994. Localization of NADPH cytochrome P450 oxidoreductase in rat brain by immunohistochemistry and in situ hybridization and a comparison with the distribution of neuronal NADPH-diaphorase staining. *Neurosci* **61**, 331-350

50. Peunova N and Enikolopov G. 1995. Nitric oxide triggers a switch to growth arrest during differentiation of neuronal cells. *Nature* **375**:68-73

51. Roskams AJ, Bredt DS, Dawson TM and Ronnett GV. 1994. Nitric Oxide Mediates the Formation of Synaptic Connections in Developing and Regenerating Olfactory Receptor Neurons. *Neuron* **13**:289-299

52. Sakashita H, Moriizumi T, Ito M, Furukawa M, Kawano J, Okoyama S, Kitao Y and Kudo M. 1995. Differentiation of the olfactory epithelium during development. *Acta Otolaryngol* **115**:93-98

53. Sanhueza M and Bacigalupo J. 1999. Odor suppression of voltage-gated currents contributes to the odor-induced response in olfactory neurons. *Am J Physiol Cell Physiol* **277**:C1086-1099

54. Sanhueza M, Schmachtenberg O and Bacigalupo J. 2000. Excitation, inhibition and suppression by odors in isolated toad and rat olfactory receptor neurons. *Am J Physiol Cell Physiol* **279**:C31-39

55. Schild D and Restrepo D. 1998. Transduction Mechanisms in Vertebrate Olfactory Receptor Cells. *Phys Rev* **78**:429-466

56. Schild D. 1989. Whole-cell currents in olfactory receptor cells of *Xenopus laevis*. *Exp. Brain Res* **78**:223-232

57. Spessert R, Wohlgemuth C, Reuss S and Layes E. 1994. NADPH-diaphorase Activity of Nitric Oxide Synthase in the Olfactory Bulb: Co-factor Specificity and Characterization Regarding the Interrelation to NO Formation. *J Histochem Cytochem* **42**:69-575

58. Stamler JS, Toone EJ, Lipton SA and Sucher NJ. 1997. (S)NO Signals: Translocation, Regulation, and a Consensus Motif. *Neuron* **18**:691-696

59. Van Wagenen S and Reeder VV. 1999. Regulation of neuronal growth cone filopodia by nitric oxide. *J Neurobiol* **39**:168-185

60. Van Wagenen S and Reeder VV. 2001. Regulation of neuronal growth cone filopodia by nitric oxide depends on soluble guanylyl cyclase. *J Neurobiol* **46**:206-219

61. Weiler E and Farbman AL. 1997. Proliferation in the Rat Olfactory Epithelium: Age-Dependent Changes. *J Neurosci* **17**:3610-3622

62. Wenisch S, Adressen C, Derouiche A, Arnhold S, Addicks K and Leiser R. 2000. Heme oxygenase-2 and nitric oxide synthase immunoreactivity of bovine olfactory receptor neurons and a comparison with the distribution of NADPH-diaphorase staining. *Histochem J* **32**:381-388

63. Zhao H, Firestein S and Greer CA. 1994. NADPH-diaphorase localization in the olfactory system. *Neuroreport* **6**:149-152